SKB TECHNICAL REPORT 85-06

Mechanical properties of granitic rocks from Gideå, Sweden

Christer Ljunggren
Ove Stephansson
Ove Alm
Hossein Hakami
Ulf Mattila

Div of Rock Mechanics
University of Luleå

Luleå, Sweden, October 1985

MECHANICAL PROPERTIES OF GRANITIC ROCKS
FROM GIDEÅ, SWEDEN

Christer Ljunggren
Ove Stephansson
Ove Alm
Hossein Hakami
Ulf Mattila

Div of Rock Mechanics
University of Luleå
Luleå, Sweden, October 1985

MECHANICAL PROPERTIES OF GRANITIC ROCKS
FROM GIDEÅ, SWEDEN

By

Christer Ljunggren
Ove Stephansson
Ove Alm
Hossein Hakami
Ulf Mattila

Div of Rock Mechanics
University of Luleå
Luleå, Sweden

ABSTRACT

The elastic and mechanical properties were determined for two
rock types from the Gideå study area. Gideå is located approximately
30 km north-east of Örnsköldsvik, Northern Sweden. The rock types that
were tested were migmatitic gneiss and migmatitic granite.

The following tests were conducted:

- sound velocity measurments
- uniaxial compression tests with acoustic emission recording
- brazilian disc tests
- triaxial tests
- three point bending tests

All together, 12 rock samples were tested with each test method. Six
samples of these were migmatitic gneiss and six samples were migma-
titic granite.

The result shows that the migmatitic gneiss has varying strength
properties with low compressive strength in comparison with its high
tensile strength. The migmatitic granite , on the other hand, is found
to have parameter values similar to other granitic rocks.

SUMMARY

This report contains the elastic and mechanical properties determined
for two rock types from Gideå, one of the chosen study areas. Gideå is
located about 30 km northeast of Örnsköldsvik. It should be pointed
out that the study of the properties is limited to intact rock. All
the tests were conducted on drill cores from corehole Gi 1 (AKGI
01000). The rock types that were tested were migmatitic gneiss and
migmatitic granite.

The following tests were conducted:

- Sound velocity measurements: dynamic elastic modulus (E_d), dynamic
  Poisson's ratio (ν_d), bulk modulus (B_d),
  primary and shear wave velocities and
  the intensity of microfracturing.

- Uniaxial compression testing: static elastic modulus (E_s), static
  Poisson's ratio (ν_s), uniaxial
  compressive strength (σ_c) and brittle-
  ness.

- Brazilian disc testing: tensile strength (indirect test).

- Triaxial testing: elastic modulus (E) and compressive strength (σ_c).

- Three point bending test: fracture toughness (K_{Ic}), elastic modulus
  (E_b) and energy release rate (G).

The results were quite average compared to other granitic rocks. The
modulus of elasticity varied between 50 - 65 GPa for both rock types
and Poisson's ratio between 0.08 - 0.33, depending on which method
that was used. The uniaxial compression strength for migmatitic gneiss
was low, (128 MPa), while it's tensile strength was comparatively
high, (18.1 MPa). The strength values for migmatitic granite were 201
MPa and 12.3 MPa respectively, which are normal values for granitic

rocks.

Results from the triaxial test show an increase in failure stress from confining pressure of 10 - 25 MPa. In particular at 25 MPa confining pressure the failure stress approaches a value which is twice that of uniaxial testing.

The fracture toughness is seen to be normal for migmatitic gneiss, while migmatitic granite is somewhat more fracture resistant than what is considered normal for granitic rock types.

TABLE OF CONTENTS

1   INTRODUCTION

A quantitative risk analysis for a final repository given a fixed locality requires access to site specific data regarding the physical characteristics of the rock mass. These data concerns fracture zones, and the hydrological characteristics of the rock mass, as well as the mechanical characteristics of the rock types contained within the rock mass.

Studies of the different type localities are based on a standard program composed of the following phases:

1) reconnaissance to chose a suitable locality
2) surface investigations
3) drillhole investigations
4) evaluation and modelling

After a non-biased evaluation and comparison of a large number of possible areas, a smaller number of sites are chosen for reconnaissance level geological and geophysical studies. The results from these studies are utilized to classify the areas. The most interesting areas warrant a reconnaissance borehole to obtain an idea of the rock mass's characteristics at depth. An evaluation is then conducted with all the previously collected information to determine which areas are interesting enough to warrant further investigation.

This report contains a summary of the elastic and mechanical properties determined for rock types taken from Gideå, one of the chosen study areas. The strength and mechanical characteristics of the rocks, as well as the in-situ stresses, are important factors in the choice of locality, construction of the storage facility, and the final deposition storage of radioactive waste. This study of rock types from Gideå is the first of its type and embraces a near complete evaluation of the elastic, dynamic, and mechanical properties of the rocks. It must, however, be pointed out that the study is limited to intact rock. No studies have been conducted concerning fractures and

discontinuities or the effects of heating on these properties.

This report contains the results from the following tests:

Sound velocity measurement: dynamic elastic modulus (E_d), dynamic Poisson's ratio (ν_d), bulk modulus (B_d), primary and shear wave velocities, and the intensity of microfracturing.

Uniaxial compression testing: static elastic modulus (E_s), (with acoustic emission) static Poisson's ratio (ν_s), uniaxial compressive strength, (σ_c), and brittleness.

Brazilian disc testing: tensile strength, (σ_t), (indirect test).

Triaxial testing: elastic modulus (E) and uniaxial compressive strength (σ_c).

Three point bending test: fracture toughness (K_{Ic}), elastic modulus (E_b), and energy release rate (G).

2   TEST SITE DESCRIPTION

2.1   Location and topography

The Gideå study area is located in northern Ångermanland approximately
30 km north-east of Örnsköldsvik (Figure 2-1). The area is situated
on a more than 100 km^2 plateau about 100 m above sea level. The study
area itself is a smaller plateau with relatively flat topography.
Elevation within the area vary between 80 m to 130 m above sea level.
The topography of the area is shown in Figure 2-2.

The locality is forested and includes small swamps. A somewhat larger
swamp is located in the north-east portion of the area. This swamp,
however, lies mainly outside the detail study area. The soil is
mainly of moraine origin and commonly overlain with peat in topograph-
ical hollows. Approximately 15% of the area is exposed bedrock.
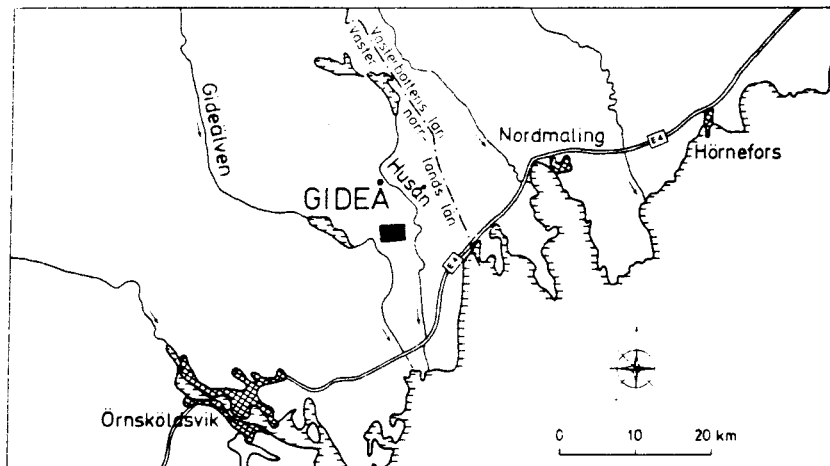
Figure 2-1, Overview map of the Gideå study area

2.2   Geology

The main rock type within the study area is banded gneiss. It is
characteristically composed of veins, schlieren and other irregular
bodies with varying mineral composition. These veins and schlieren are

generally north-east striking with a general dip of 10^0 to 20^0 to the north-west.

The mineral assemblage of the banded gneiss is quartz (56%), biotite (19%), plagioclase (13%), and microcline (6%). Sulfide minerals are present in small amounts of which the most common is pyrrohtite appearing as small clusters in the matrix or as fracture fillings. The content of ore minerals is so low that mining will never be economically feasible.

Occasionally, granitic gneiss is found within the study area. Even this rock type has been affected by the alteration and deformation that affected the banded gneiss. Granitic gneiss appears as thin horizontal layers parallel with the structure of the banded gneiss and composes 6% of the total core length.
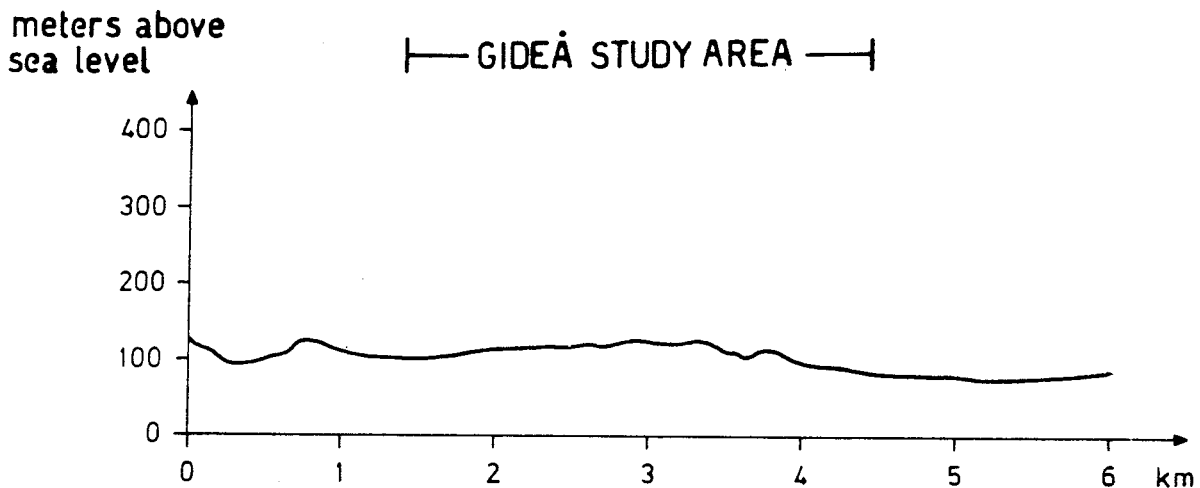
Figure 2-2 Topographic profile through the Gideå study area. Profile is east - west striking.

2.3   Corehole Gi 1

All the testing within this study was conducted on drill core from corehole Gi 1 (AKGI01000). The rock types that were tested were migmatitic gneiss (migmatite) and migmatitic granite (aplite granite).

Corehole Gi 1 is vertical and has a length of 704.25 m. The hole indicates that migmatite is predominant, at least to a depth of 700 m. If the migmatite is divided into migmatitic gneiss and migmatitic granite, the following percentages are obtained: migmatitic gneiss (90%), migmatitic granite (6.0%), pegmatite (3.5%), and diabase (0.5%).

The migmatite is fine to medium grained and have a massive texture. Colour varies between grey white and grey black. The material is occasionally porphyritic with feldspar eyes 3 - 10 mm in size. The migmatite is often foliated and even folded. Locally, the rock is rich with sedimentary material - up to 50% of the mineral content. Granitic material appears as small bodies within the larger rock mass. The most common minerals are feldspar, quartz and biotite.
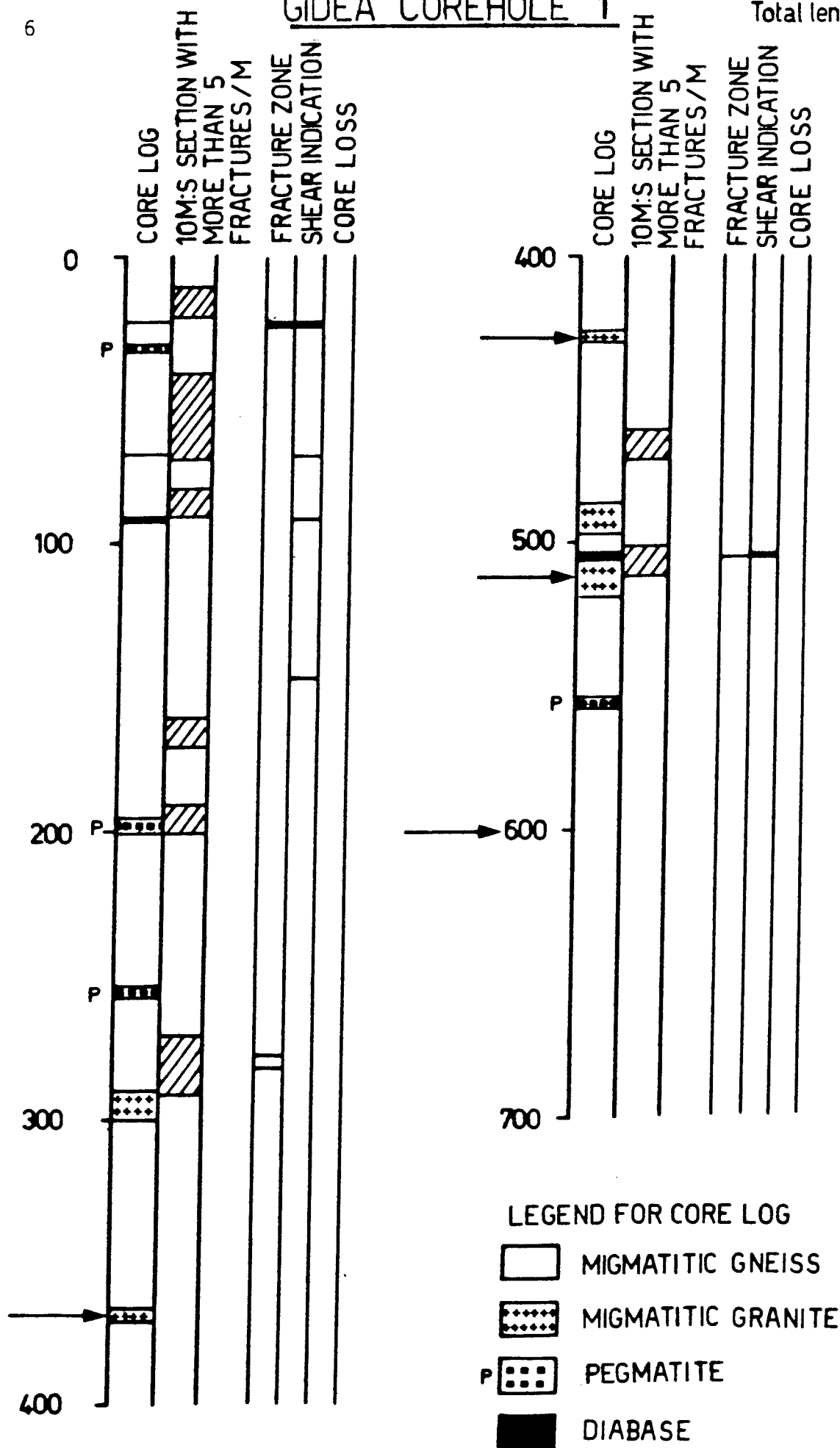
Figure 2-3 Summary of core mapping for drillhole Gi 1. Arrows indicate from which depths the test samples were taken. After Albino, et. al., 1982

3   RESULTS

The following tests were conducted:

- sound velocity measurements

- uniaxial compression tests with acoustic emission recording

- brazilian disc tests

- triaxial tests

- three point bending tests

All together, 12 rock samples were tested with each test method. Of these, 6 samples were migmatitic gneiss (migmatite) and 6 samples migmatitic granite (aplite granite).

The preparation of the samples for testing will not be discussed in this section. A discussion describing sample preparation for the test methods is located in Appendix 1-6.

3.1 Sound velocity measurements

A summary of the results from the sound velocity testing giving values for the dynamic elastic modulus (E_d), dynamic Poisson's ratio (ν_d), bulk modulus (B_d), primary and shear wave velocities, and a measure of the microfracture intensity (V_s/V_p) is given as Table 3-2. Table 3-1 displays the classification of microfracturing intensity from sound velocity ratio (V_s/V_p) proposed by Torenq et al. (1971).

Table 3-1 Classification of microfracturing intensity (Torenq et al. 1971)

Vs/Vp	Classification
<0.6	unfractured
0.6 - 0.7	some microfractures
>0.7	highly microfractured

Table 3-2: Results from sound velocity measurements conducted on rock samples from Gideå

Rocktype	Vp m/s	Vs m/s	Vs/Vp	E-mod (GPa)	ν	B-mod (GPa)
Gneiss 1	5768	3390	0.59	76.6	0.236	48.4
" 2	5598	3540	0.63	79.2	0.167	39.6
" 3	4686	3426	0.73	59.2	neg	17.2
" 4	4559	3202	0.70	56.8	0.013	19.4
" 5	4519	3222	0.71	56.0	neg	18.0
" 6	4879	3335	0.68	64.4	0.061	24.4
Average Std.dev.	5000 ±545	3350 ±128	0.67 ±0.05	65.4 ±10.2	0.12 ±0.1	27.8 ±13.1
Granite 1	4816	2952	0.61	55.1	0.199	30.5
" 2	4729	3020	0.64	55.4	0.155	26.8
" 3	4856	3193	0.66	60.1	0.119	26.3
" 4	4462	3080	0.69	52.2	0.045	19.1
" 5	4640	2949	0.64	53.3	0.161	26.2
" 6	4816	3138	0.65	58.8	0.131	26.5
Average Std.dev.	4720 ±148	3055 ±100	0.65 ±0.03	55.8 ±3.1	0.135 ±0.05	25.9 ±3.7

3.2 Uniaxial compression testing with simultaneous acoustic emission recording

The rock types' static elastic moduli (E_s), static Poisson's ratio (v_s), and uniaxial compressive strength were determined with this test. The acoustic emissions (AE) generated by the samples during testing were monitored continuously. These acoustic emission results give an understanding of at what loads microfracturing begins in the sample. They can also be utilized for a general classification of the brittleness of the rocks. A histogram showing the compressive strength of the individual specimens is displayed in figure 3-1. Typical curves for migmatitic gneiss and migmatitic granite showing stress plotted versus radial and axial strain are shown in Figure 3-2. The results from the uniaxial compression testing are summarized in table 3-3. A description of the test method is found in Appendix 2.
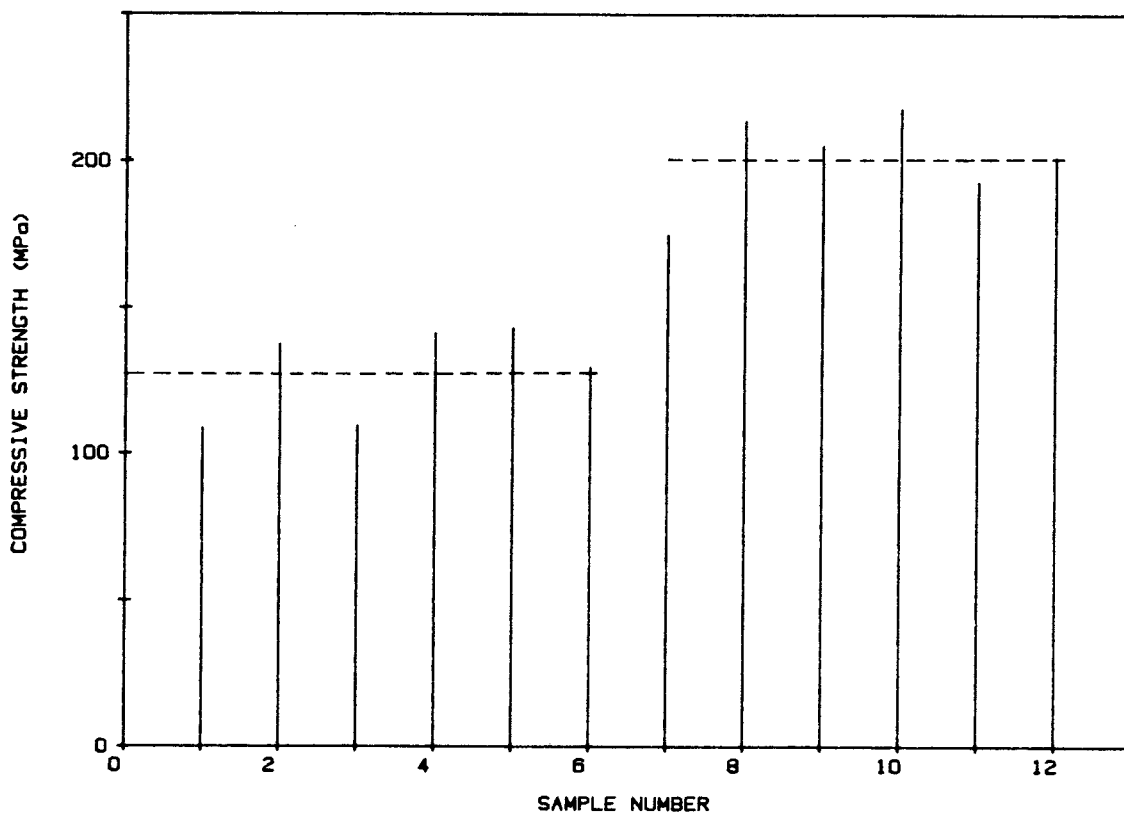
Figure 3-1 Results from uniaxial compression tests. Sample number 1-6: migmatitic gneiss, sample number 7-12: migmatitic granite
The dotted line indicates the average value for each rock type

Table 3-3 Results from uniaxial compression testing on Gideå samples

Rocktype	ϕ (mm)	L (mm)	m (g)	ρ (kg/m^3)	E_s^{i} * (GPa)	ν_s^{i} *	E_s^{50} ** (GPa)	ν_s^{50} **	SP (%)	σ_c (MPa)
Gneiss 1	41.4	104.4	378.7	2695	53.1	0.16	58.5	0.20	----	108.6
" " 2	41.2	103.0	371.7	2707	17.7	0.05	62.7	0.26	63.7	137.5
" " 3	41.4	104.5	383.5	2726	33.9	neg.	53.8	0.21	65.7	109.5
" " 4	41.4	104.4	383.9	2732	34.9	0.13	56.2	0.33	68.1	141.2
" " 5	41.4	104.4	385.4	2742	41.9	0.08	51.0	0.25	90.3	142.9
" " 6	41.4	104.4	383.1	2726	40.4	0.11	56.4	0.22	71.4	129.5
Average	----	-----	-----	----	37.0	0.11	56.4	0.24	71.8	128.2
Std.dev.	----	-----	-----	----	±11.7	±0.04	±4.0	±0.05	±10.7	±15.5
Granite 1	41.4	104.5	370.9	2637	36.5	0.12	63.9	0.33	50.6	174.7
" " 2	41.5	104.5	371.5	2628	39.3	0.09	65.3	0.29	33.6	213.7
" " 3	41.6	104.4	373.7	2634	40.2	0.10	67.7	0.35	41.7	205.3
" " 4	41.5	104.4	371.7	2632	32.3	0.05	66.8	0.39	38.3	217.9
" " 5	41.6	104.4	374.4	2639	25.9	neg.	52.6	0.24	49.5	192.9
" " 6	41.5	104.5	373.0	2639	38.4	0.06	69.3	0.30	51.2	201.3
Average	----	-----	-----	----	35.4	0.08	64.3	0.32	44.2	201.0
Std.dev.	----	-----	-----	----	±5.4	±0.03	±6.0	±0.05	±7.4	±15.6

* E_s^{i} and ν_s^{i} are calculated at initial load
** E_s^{50} and ν_s^{50} are calculated at 50% of compressive strength
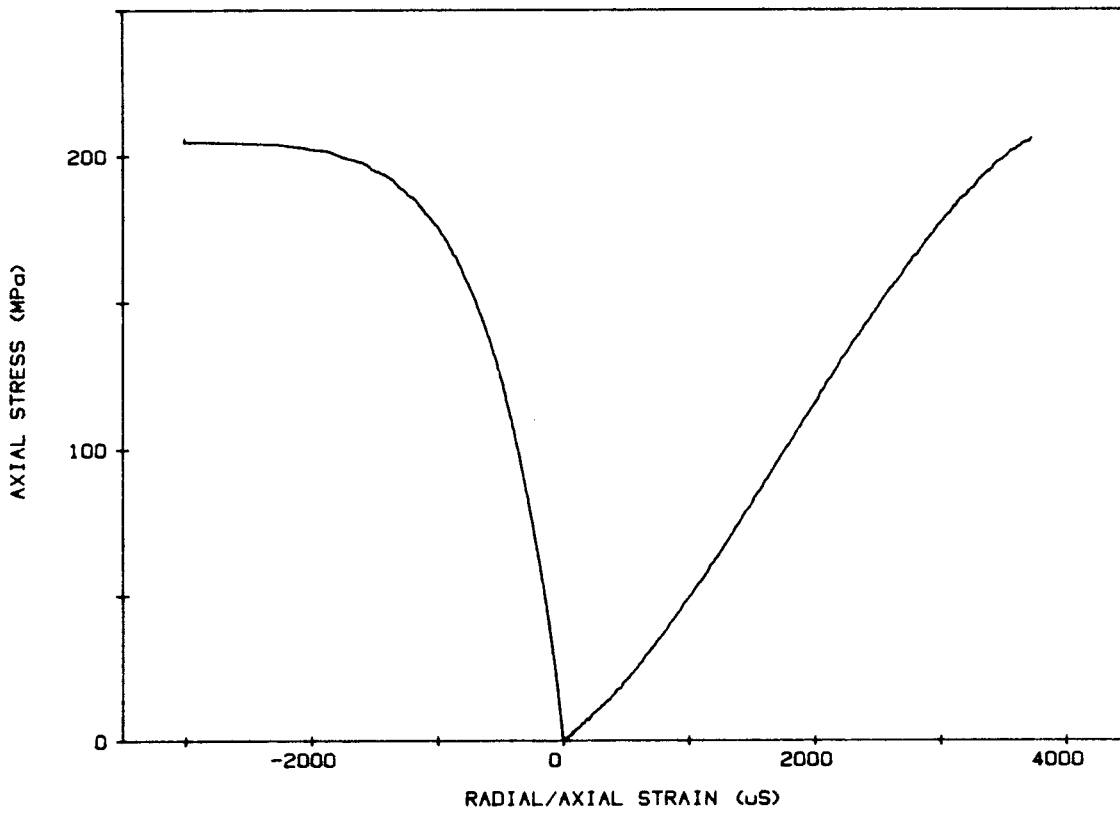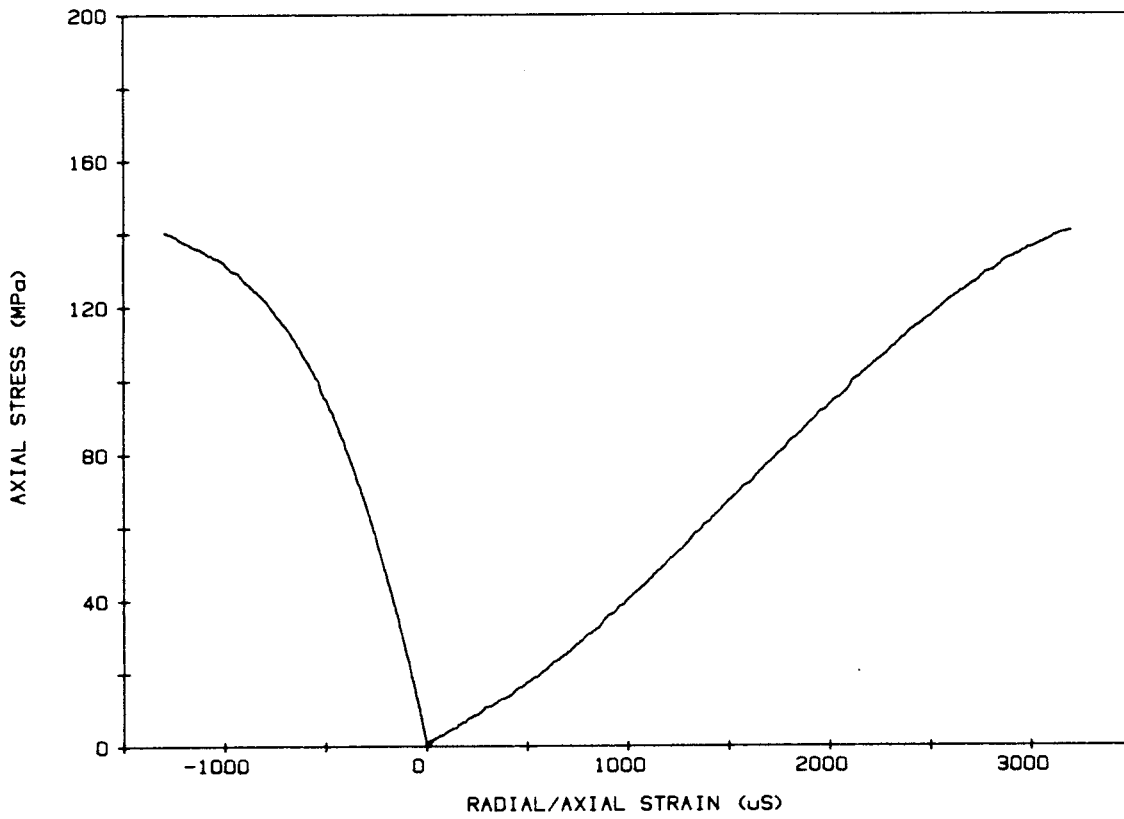
Figure 3-2 Stress versus radial/axial deformation
A) migmatitic gneiss, B) migmatitic granite

SP is a measure of the brittleness of the rock. It is determined by the shape of the acoustic emission curve. SP is defined as:

$$SP = F_{sp}/F_{max}$$

Where: F_{sp} = the load when the number of acoustic events in two seconds is equal to 1000

F_{max} = failure load

A classification of the brittleness given the SP value is given in Table 3-4. Typical acoustic emission curves from both of the tested rock types are shown in Figure 3-3. The solid line in the figures are arrived at by a curve fitting procedure in order to allow SP to be determined. The methodology for the registration of AE is described in Appendix 3.

Table 3-4 Classification of rock brittleness, SP
        (after Ljunggren, Norin, 1985)

SP	Classification
>0.9	very brittle
0.7 - 0.9	brittle
0.5 - 0.7	ductile
<0.5	very ductile
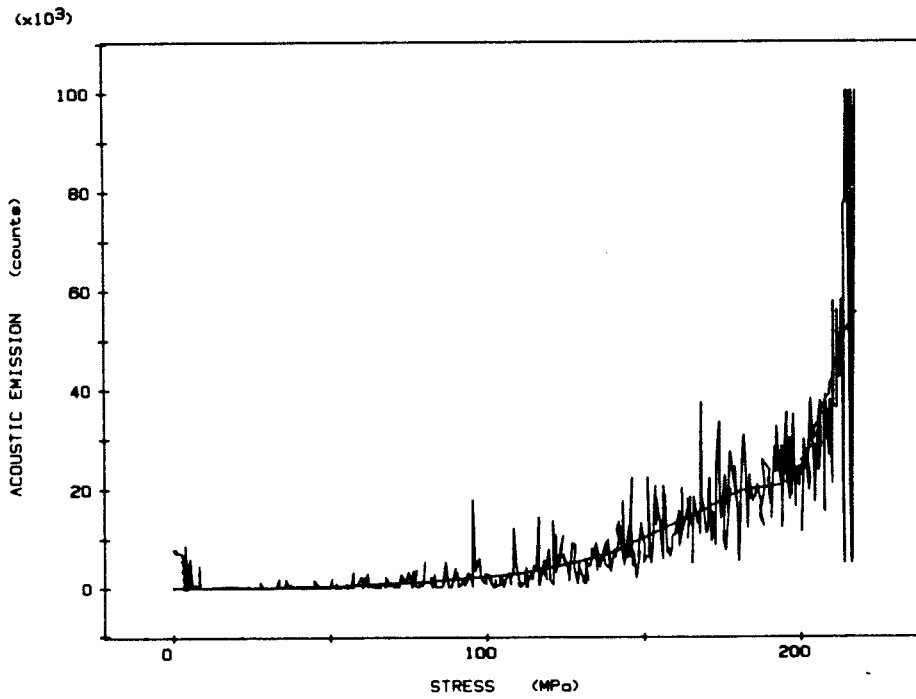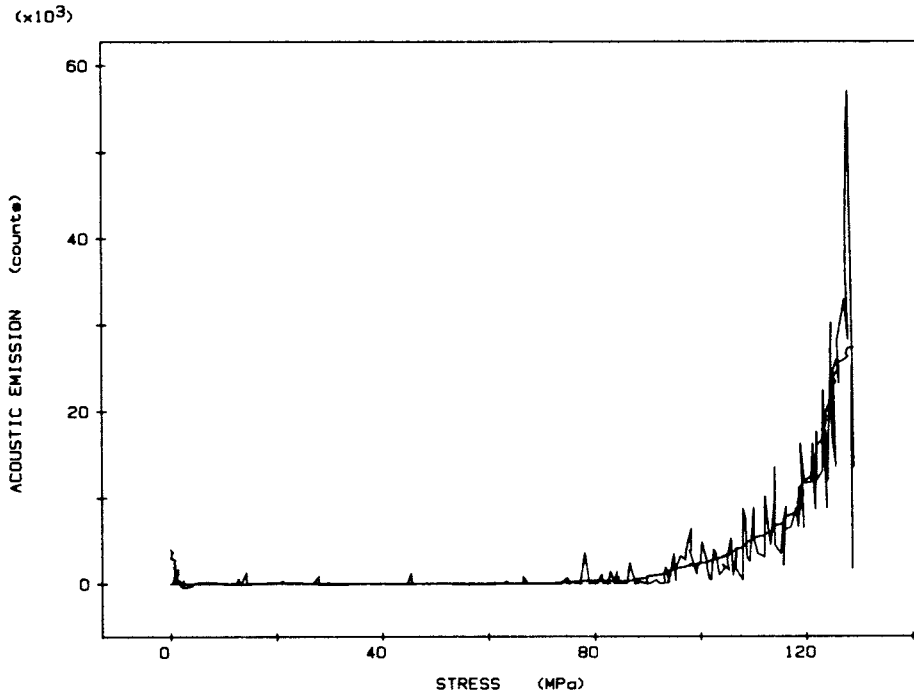
Figure 3-3 Acoustic emission versus axial stress for uniaxial compression test. A: migmatitic gneiss, B: migmatitic granite

3.3   Brazilian disc test

The tests were conducted on 12 disc shaped rock samples. Calculated tensile strengths are shown in Table 3-5 and Figure 3-4. The test procedure is described in Appendix 4.

Table 3-5 Brazilian disc test results, Gideå

Rocktype	Φ (mm)	L (mm)	Mass (g)	Density (kg/m³)	σ_t (MPa)
Gneiss 1	41.4	21.2	76.7	2688	21.3
" 2	41.3	21.1	76.5	2706	17.3
" 3	41.5	21.1	77.5	2715	13.8
" 4	41.5	21.1	77.5	2715	15.3
" 5	41.4	21.1	77.7	2736	21.5
" 6	41.4	21.2	77.6	2719	19.5
Average	----	----	----	2713	18.1
Std.dev.	----	----	----	±15.8	±3.2
Granite 1	41.4	21.0	74.6	2641	12.8
" 2	41.5	21.1	74.8	2621	13.9
" 3	41.6	21.1	75.3	2626	12.1
" 4	41.5	21.2	75.3	2626	12.1
" 5	41.6	21.1	75.8	2643	9.2
" 6	41.5	21.3	76.0	2638	13.5
Average	----	----	----	2632	12.3
Std.dev.	----	----	----	±9.3	±1.7
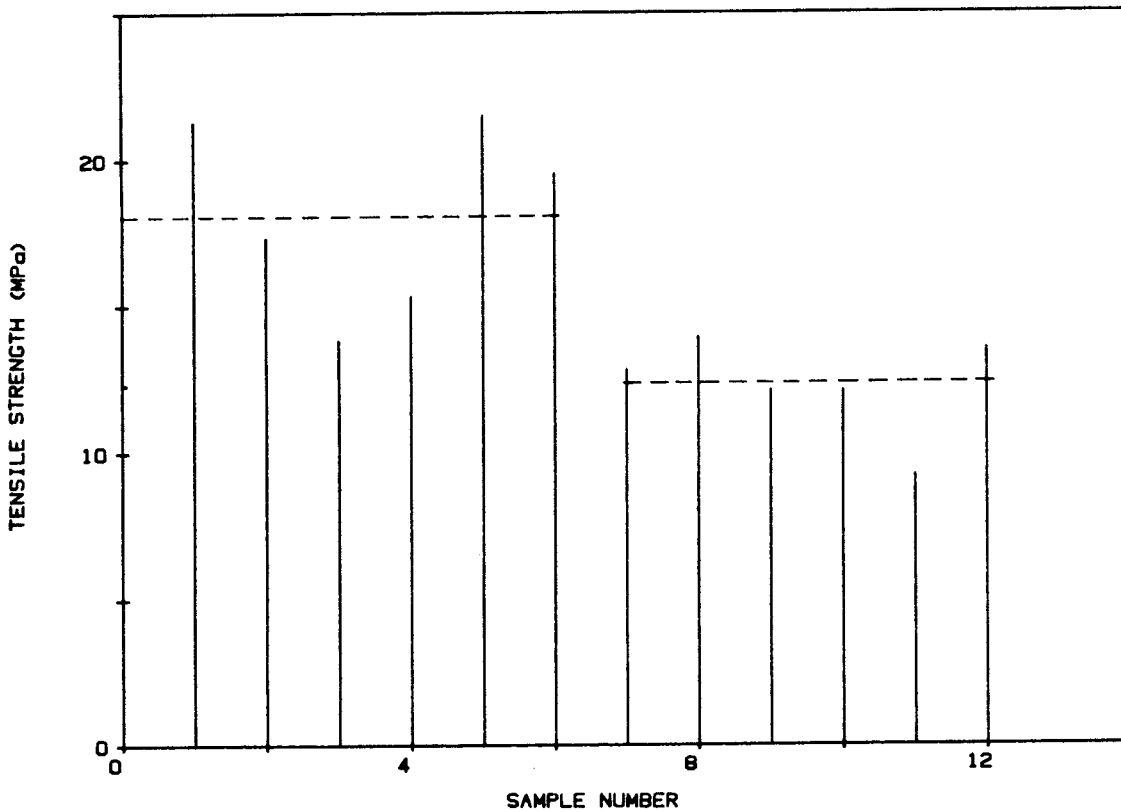
Figure 3-4 Brazilian disc test results.

       Sample number 1-6; migmatitic gneiss

       Sample number 7-12; migmatitic granite

       The dotted line indicates the average value for each rock type

3.4   <u>Controlled triaxial testing</u>

Samples of the rocks tested were taken from a depth of 599m to 606m. A total of six samples were tested with three different confining pressures. Results from the testing are given as Table 3-6. Figure 3-5 shows a typical load-deformation curve at 10 MPa confining pressure.
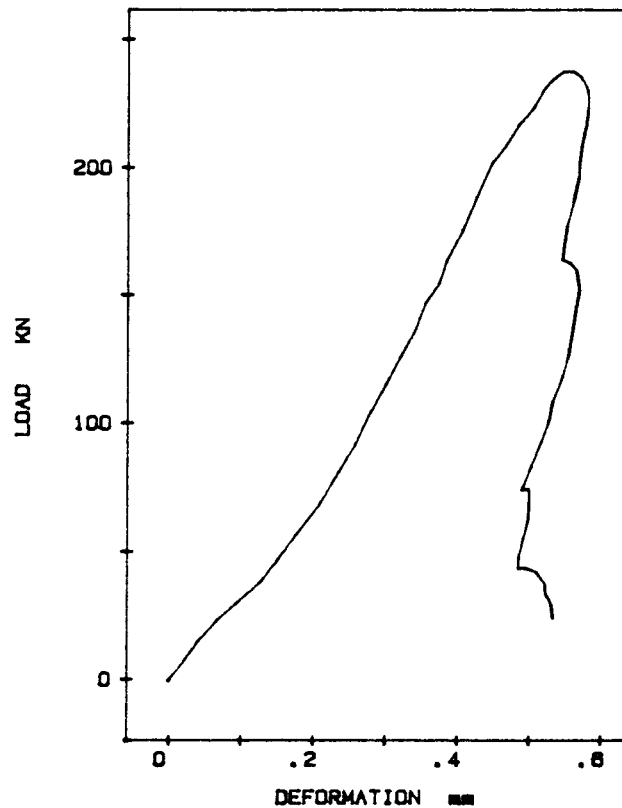
Figure 3-5 A typical load-deformation curve at a confining pressure of 10 MPa. Sample Gid 3(10).

As it can be seen, the curve continues to have a positive slope after the peak load has been passed. This type of behaviour is well known for most of hard and brittle rocks and is called 'a class two' behaviour according to the classification of Waversik,1968. The testing procedure and equipment are described in Appendix 5.

Table 3.6 Results from controlled triaxial testing on migmatitic gneiss, Gideå study area.

Confining Pressure (MPa)	Sample No	Fracture Stress (MPa)	Young's Modulus (GPa)	Failure Description
5	Gid 1(5)	147.2	61.4	Well defined oblique fracture plane
5	Gid 2(5)	162.4	59.8	
10	Gid 3(10)	240.4	63.8	"
10	Gid 4(10)	181.9	64.2	"
25	Gid 5(25)	357.2	68.4	"
25	Gid 6(25)	295.6	66.7	"

3.5   Three point bending test

The tests were conducted according to the SENRBB (single edge round bar bending) method. That is, the samples were prepared with a straight notch which acted as a fracture initiator. With this test, Poisson's ratio must be known to calculate the mechanical failure properties. The fracture mechanical parameters, K and G, have been calculated using two different values of Poisson's ratio, n_s^i and n_s^{50}, which were obtained from the uniaxial compression tests. As is seen in table 3-7 and 3-8 the value of the Poisson's ratio has a very limited impact on the values of K and G. The testing procedure and equipment are described in Appendix 6.

table 3-7 Three point bending test results, Gideå
Calculations conducted with v_s^i

Rocktype	Φ (mm)	$\dfrac{a_0}{\Phi}$	E-mod (GPa)	$\dfrac{a}{\Phi}$	F_{max} (kN)	K $(MN/m^{3/2})$	G (J/m^2)
Gneiss 1	41.5	0.241	55.5	0.349	2.33	2.083	77.3
" 2	41.5	0.241	53.9	0.331	2.29	1.951	69.8
" 3	41.6	0.240	46.6	0.276	1.69	1.241	32.7
" 4	41.3	0.242	60.3	0.393	2.18	2.228	81.3
" 5	41.5	0.241	27.7	0.359	1.35	1.241	54.9
" 6	41.4	0.242	63.1	0.335	2.77	2.394	89.8
Average Std.dev.	---- ----	---- ----	51.2 ±12.8	---- ----	2.10 ±0.50	1.86 ±0.50	67.6 ±20.8
Granite 1	----	----	-----	----	----	---------	------
" 2	41.6	0.240	63.4	0.355	3.11	2.819	124.3
" 3	41.6	0.240	60.9	0.371	3.19	3.025	149.0
" 4	41.5	0.241	52.7	0.367	2.89	2.722	139.5
" 5	41.5	0.241	46.5	0.330	2.40	2.039	89.2
" 6	41.5	0.241	36.9	0.394	1.95	1.985	106.4
Average Std.dev.	---- ----	---- ----	52.1 ±10.8	---- ----	2.71 ±0.52	2.52 ±0.48	121.7 ±24.3

Table 3-8 Three point bending test results, Gideå
Calculations conducted with v_s^{50}

Rocktype	Φ (mm)	$\dfrac{a_0}{\Phi}$	E-mod (GPa)	$\dfrac{a}{\Phi}$	F_{max} (kN)	K $(MN/m^{3/2})$	G (J/m^2)
Gneiss 1	41.5	0.241	55.6	0.354	2.33	2.110	75.2
" 2	41.5	0.241	54.0	0.334	2.29	1.967	67.4
" 3	41.6	0.240	46.7	0.276	1.69	1.241	31.0
" 4	41.3	0.242	60.4	0.400	2.18	2.269	80.0
" 5	41.5	0.241	27.8	0.363	1.35	1.256	53.5
" 6	41.4	0.242	63.2	0.338	2.77	2.413	86.6
Average Std.dev.	---- ----	---- ----	51.3 ±12.8	---- ----	2.10 ±0.50	1.88 ±0.50	65.6 ±20.4
Granite 1	----	----	------	----	----	---------	------
" 2	41.6	0.240	63.4	0.362	3.11	2.879	116.7
" 3	41.6	0.240	60.9	0.380	3.19	3.105	141.3
" 4	41.5	0.241	52.7	0.377	2.89	2.793	132.3
" 5	41.5	0.241	46.6	0.334	2.40	2.064	84.7
" 6	41.5	0.241	37.0	0.401	1.95	2.031	103.2
Average Std.dev.	---- ----	---- ----	52.1 ±10.8	---- ----	2.70 ±0.52	2.57 ±0.49	115.6 ±22.6
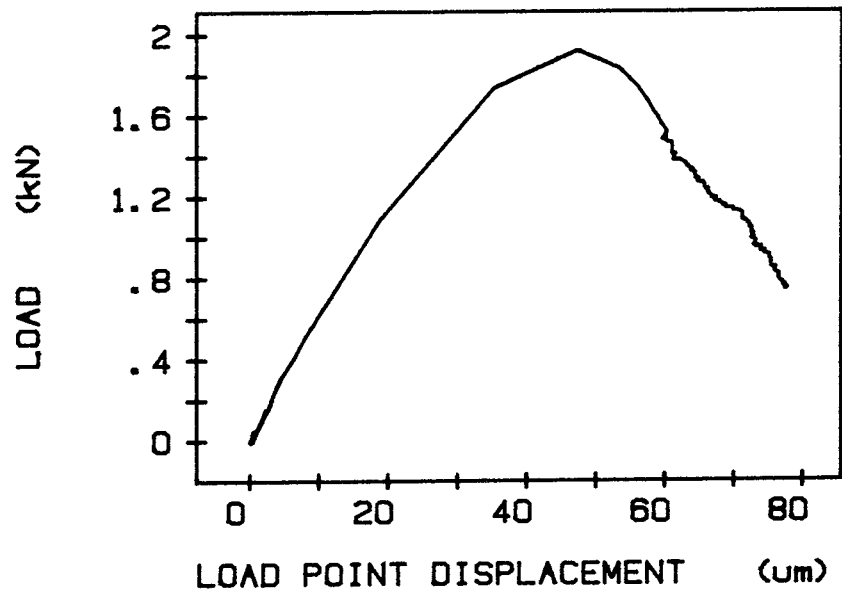
Figure 3-6 Typical recording from three point bending test.
Migmatitic granite.

4   DISCUSSION

Primary and shear wave velocities for the Gideå rock types are high
for migmatitic gneiss and moderate for migmatitic granite when
compared with other Swedish granitic rocks. The microfracturing grade,
V_s/V_p, is typical for granitic rocks. It may also be pointed out that
the migmatitic gneiss has a higher dynamic elastic modulus than the
migmatitic granite. Results from the other tests (uniaxial
compression test and three point bending test) indicated the contrary.
A contributing factor is the higher density of the migmatitic gneiss,
as density is included in the calculation of the elastic moduli from
the sound velocity measurments. It is also notable that the
migmatitic gneiss has the lowest compressive strength, σ_c, but the
highest tensile strength, (σ_t). This may be attributed to the mineral
composition and shape of mineral grains. There is a clear shape
orientation of the mica minerals in the migmatitic gneiss, and this
has probably had some effect on the test results.

The tensile strength of the migmatitic gneiss is high while that of
the migmatitic granite is around average for granitic rock types in
Sweden. The compressive strength, σ_c, determined from uniaxial
compression testing for migmatitic granite (201 MPa) is clearly
comparable to that of Stripa granite (205 MPa) and considerably higher
than Bohus granite (157 MPa). Compressive strength of the migmatitic
gneiss for Gideå is considerably lower (128 MPa). This is most likely
due to its higher mica content. Plans cutting through a large number
of mica crystals tend to act as weakness planes.

The brittleness of the migmatitic granite is comparable with that of
the Stripa granite, whereas that of the gneiss is higher. Previous
studies (Ljunggren, Norin, 1985), indicate however, that an increase
in mica content has a damping effect on the registration of acoustic
events.

Results from the controlled triaxial test show an increase in failure
stress from 10 MPa to 25 MPa confining pressure. In particular, at
25 MPa confining pressure, the failure stress approaches a value which

is double that arrived at from uniaxial testing. Due to material variation and the limited number of samples tested, it is not possible to distinguish any change in failure stress up to 5 MPa confining pressure.

Young's moduli obtained from these tests are consistent with those obtained from uniaxial testing. Although a slight increase of the moduli may be expected as a result of confinement, this cannot be shown due to the limited number of samples tested.

To classify the results of the testing as objectively as possible, and to ascertain whether the strength values could be regarded as weak or strong, we have chosen to compare them with a compilation of parameters for crystalline rock types conducted by Tammemagi and Chieslar (1985). Information on Swedish rock types ((Swan, 1977) and (Swan, 1983)) is also found in this work. We have chosen to re-present their data here and, at the same time, indicate where the results from the Gideå rock types appear.

As is seen in Figure 4-1, the density values obtained from the Gideå rock types fall well within the area that can be regarded as normal for acid igneous rocks.

The compiled data on the elastic moduli exhibit a much larger standard deviation than what is found in the density data. The reason for this lies partly in the variety of test methods used and partly in the different evaluation methods. The results, however, give and adequate picture of the interval within which the elastic moduli normally are located.
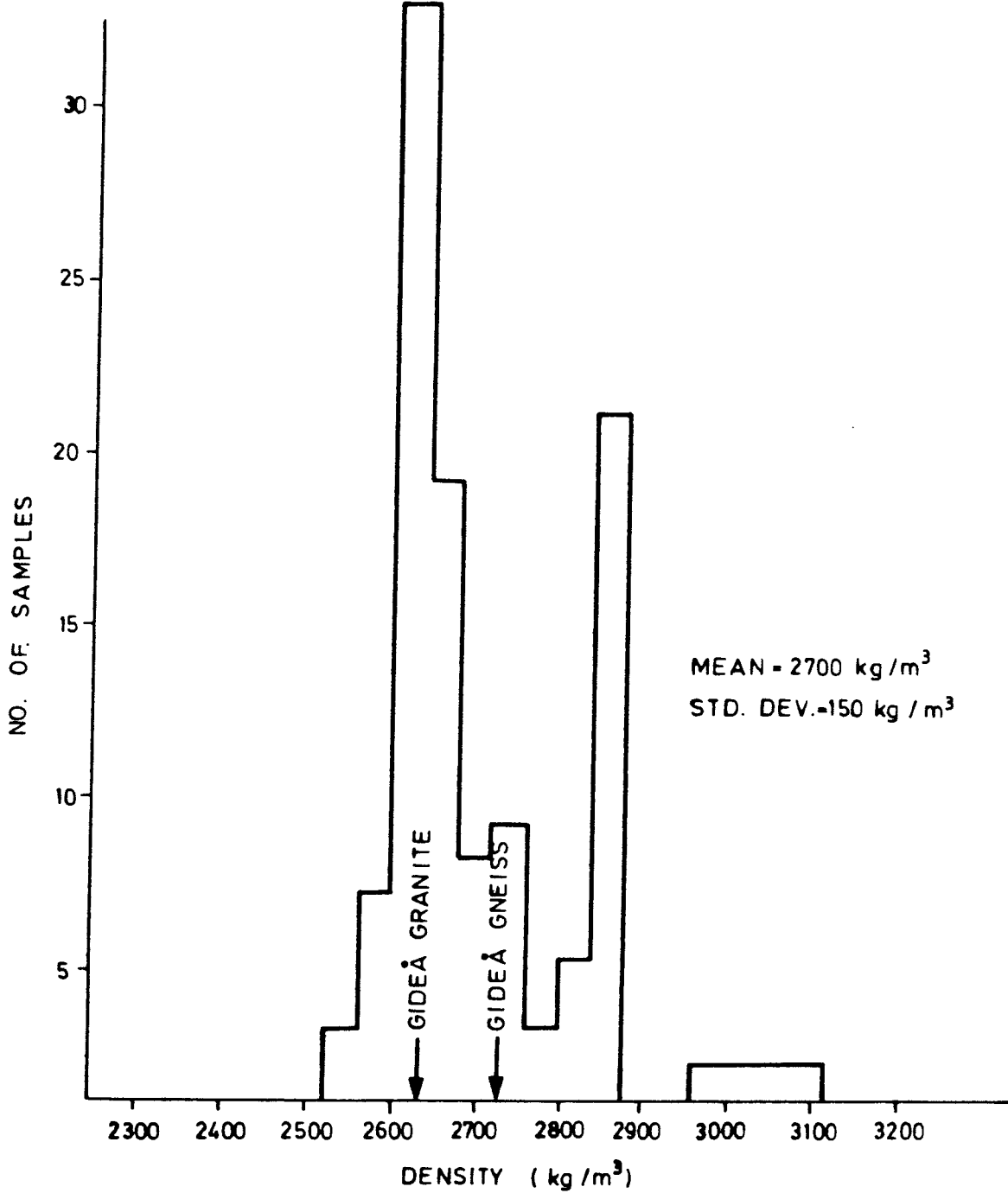
Figure 4-1 Frequency histogram of density of crystalline rocks. 104 samples. Gideå results are indicated by the arrows. (After Tammemagi and Chieslar, 1985).
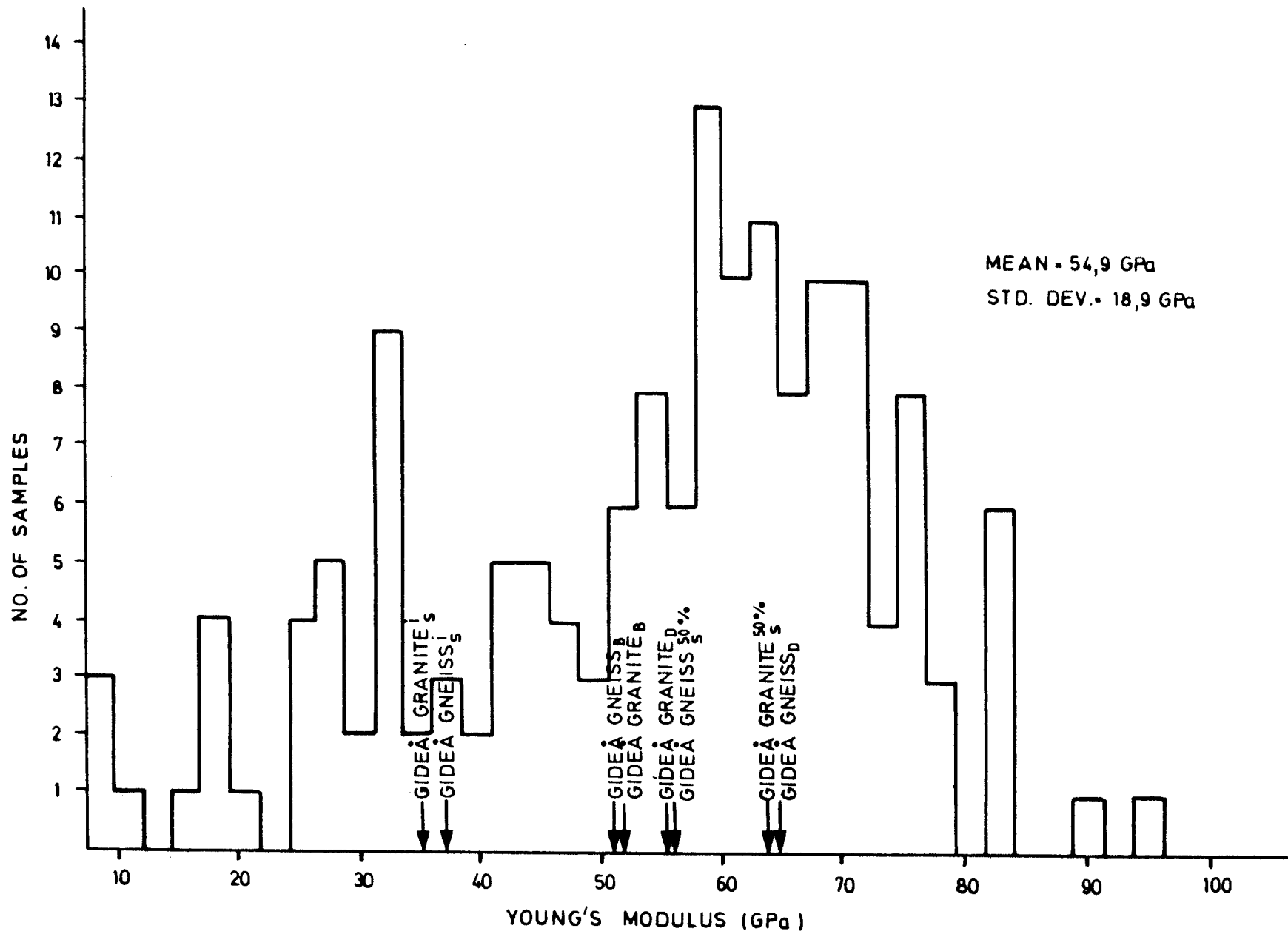
Figure 4-2 Frequency histogram of Young's modulus for crystalline rocks. 160 samples. Results from Gideå are indicated by the arrows. (After Tammemagi and Chieslar, 1985).

As is seen in Figure 4-2, the initial elastic moduli, obtained from uniaxial compression testing, E_s^i, are markedly different from the others. This is probably due to closing of microcracks and collapsing of aspherical pores. Part of the measured strain is then a result of rigid translation and rotation of crystals instead of true distortion of crystal lattices. The calculated elastic modulus will then be smaller at very low loads than at loads above which microcracks and some pores have closed. In general, the elastic moduli from the Gideå rock types lie in the vicinity of the average for the entire compilation, with the migmatitic granite having a somewhat higher value.

Poisson's ratio depends on which test and evaluation method was used to obtain the result. Generally speaking, it can be concluded that the Gideå results fall well within the area that is considered normal for crystalline rock types.

The large standard deviation (81.6 MPa) is clear evidence of the large variation that is present in the uniaxial compressive strength determinations. As is seen in Figure 4-4, there is an obvious maximum at around 200 MPa. Migmatitic granite can be taken as having a moderate average value of compressive strength while migmatitic gneiss has a considerably lower strength.

The determination of tensile strength of intact rock is a complex task. Laboratory tests invariably indicate that tensile strength depends upon sample size (the larger the sample, the lower the strength) and upon the testing method utilized. Some of the methods used for the determination of rock tensile strength are: direct tension test, Brazilian disc test, and hydraulic fracturing. Even if only one method is utilized, the data shows a large scatter about the mean. Keeping this in mind, it is, however, apparent that the tensile strength values of the Gideå samples, especially the migmatitic gneiss, are quite high.
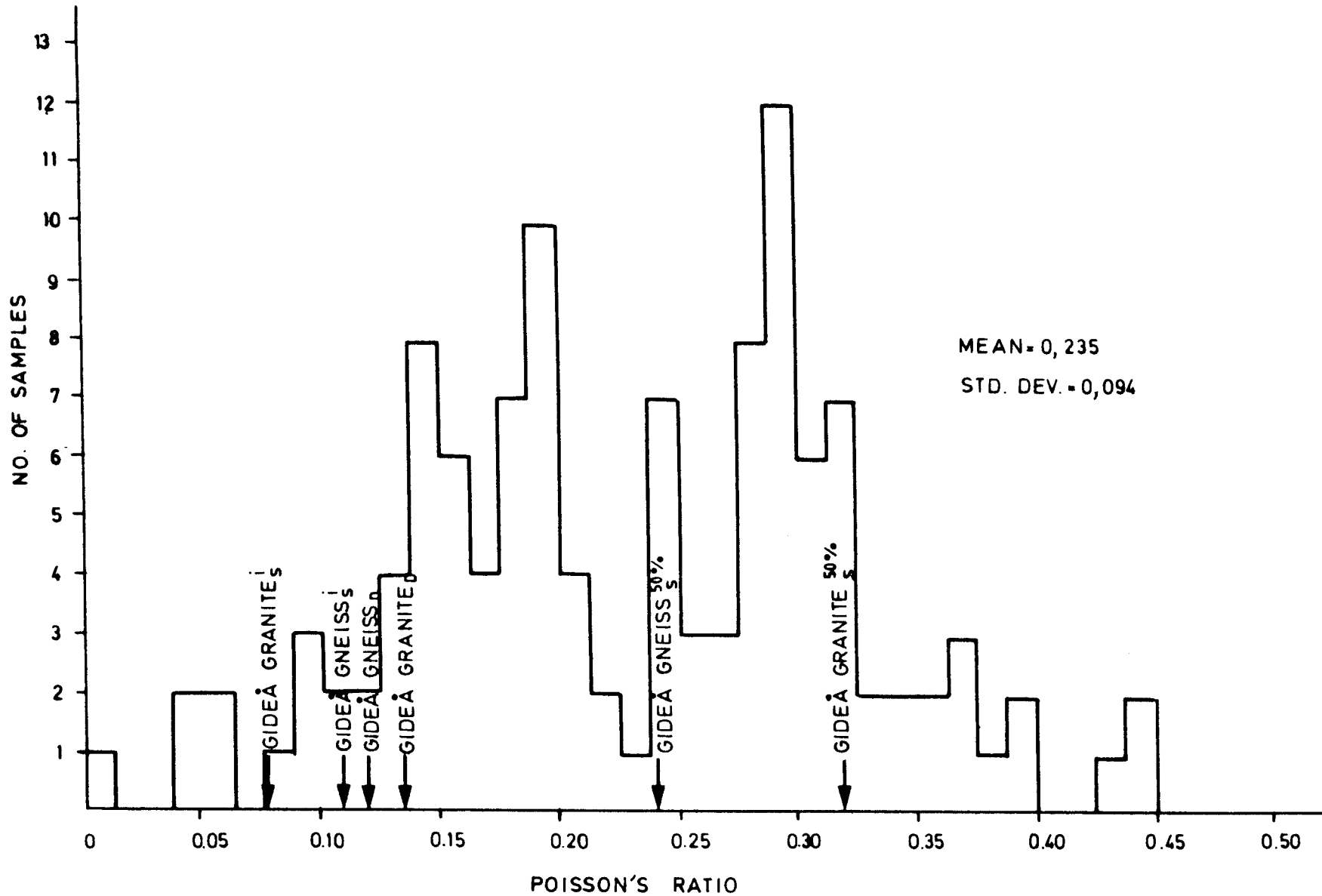
Figure 4-3 Frequency histogram of Poisson's ratio for crystalline rocks. 121 samples. Results from Gideå are indicated by the arrows. (After Tammemagi and Chieslar, 1985).
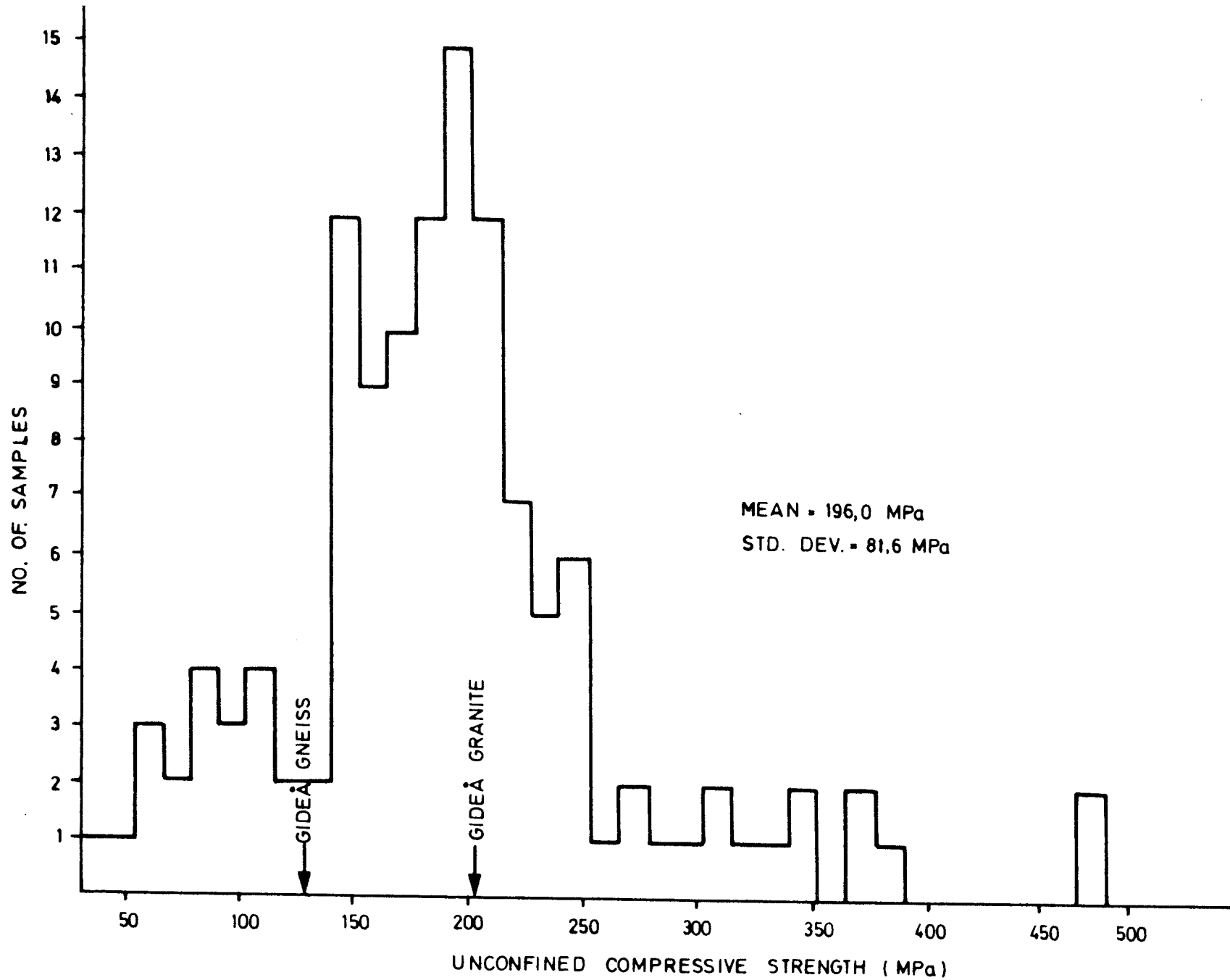
Figure 4-4 Frequency histogram of unconfined compressive strength for crystalline rocks. 127 samples. Gideå results are indicated by the arrows. (After Tammemagi and Chieslar, 1985).
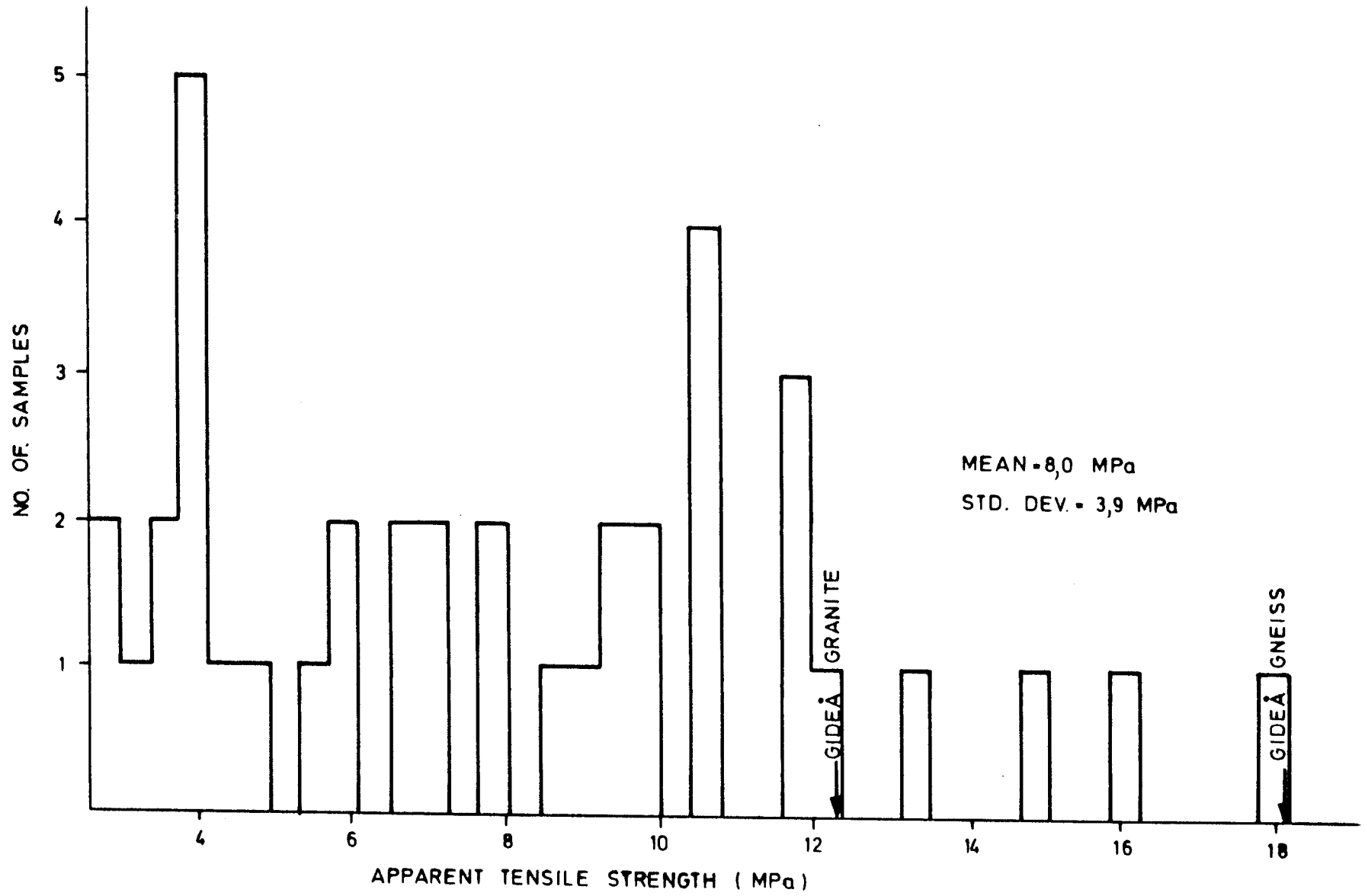
Figure 4-5 Frequency histogram of apparent tensile strength for crystalline rocks. 39 samples. Gideå results are indicated by the arrows. (After Tammemagi and Chieslar, 1985).

The fracture toughness, K_{IC}, which is described as the rock's resistance to fracture propogation, is seen to be normal for migmatitic gneiss when compared to other crystalline rock types. The migmatitic granite, which has a K_{IC}=2.52 MN/m3/2 is somewhat more fracture resistant than what is considered normal for granitic rock types (see Table 4-1).

Table 4-1 Fracture toughness for granitic rock types

Rocktype	K_{IC} $(MN/m^{3/2})$
Migmatitic gneiss, Gideå	1.88
Migmatitic granite, Gideå	2.52
Granite, Öjebyn	1.41[1]
Quartzite, Kiruna	2.28[2]
Stripa granite	1.98[3]
Avesta gneiss	1.94[4]

[1] Obtained from results reported by Lindqvist and Rånman (1980)
[2] Alm (1983)
[3] Sun (1983)
[4] Ljunggren, Norin (1985)

A final evaluation of the characteristics of the tested rock types is that the migmatitic gneiss has varying strength properties. What is especially obvious is its low compressive strength in comparison to its high tensile strength. Petrographic studies indicate that the minerals which compose the material have a preferred shape orientation and that the content of mica is significant. The latter factor has a negative effect on the compressive strength. Migmatitic granite, however, may be classed as having average values (c.f. Tammemagi and Chieslar, 1985). No data from Gideå can be regarded as abnormal.

5   RECOMMENDATIONS

To increase our knowledge of the mechanical characteristics of Swedish
rocks, and in particular those that eventually will be targets for
further development for a nuclear waste repository, it is important to
test the rock types that appear in the other study areas.

A problem that always confronts the investigator is that testing is
conducted on fresh, intact rock whereas the excavation is carried out
in a rock mass which in addition contains fractures, joints and joint
fillings. Elastic and fracture mechanical properties of intact rock
are there- fore not the same as those of a rock mass. Hence a more
complete study of rock mass characteristics must incorporate studies
of joint properties as well as the properties of the joint filling
materials. Studies along these lines are recommended before any final
design of the repository is made. A more comprehensive study of the
properties of the intact rock is also necessary.

Direct experimental studies of rock mass properties are difficult to
carry out. Nevertheless such results are of vital importance if a
better understanding of the behaviour of the rock mass is to be
reached. Large scale testing offers interesting prospects in this
case. A great step towards controlled experimental studies of rock
mass properties would be taken if specimens having dimensions of
approximately 1x1x1 m could be tested. Large scale laboratory testing
are therefore recommended for future research.

6   REFERENCES

[1] Albino B, Nilsson G, 1982. Sammanställning av tekniska data för
     de olika borrhålen samt sprick- och bergartsloggar,
     typområdet Gideå. KBS ARBETSRAPPORT AR 84-23.

[2] Albino B, Nilsson G, Stenberg L, 1982. Geologiska och geofysiska
     mark- och djupundersökningar. KBS ARBETSRAPPORT AR 83-19.

[3] Alm O, 1983. Results from Mechanical Testing of Six Different
     Rock Materials. Internrapport BM 1983:05. 30p.

[4] Hakami H, 1985. Cast On Rock Inclusion Gauged Sleeve for
     Controlled Uni-axial and Tri-axial Compression Tests on
     Rocks. A progress report, Internrapport BM 1985:01.

[5] ISRM, 1981. Rock Characterization Testing and Monitoring. ISRM
     Suggested Methods. Brown E T (Ed). 211 p.

[6] KBS-3. Använt kärnbränsle-KBS-3. II Geologi. SKBF/KBS.

[7] KBS-3: Använt kärnbränsle-KBS-3. IV Säkerhet. SKBF/KBS.

[8] Lindqvist P-A, Rånman K-E, 1980. Mechanical Rock Fragmentation;
     Chipping Under a Disc Cutter. Technical Report 1980:59 T,
     University of Luleå, Sweden.

[9] Ljunggren C, Norin J, 1985. Akustisk Emission vid Bergarts-
     testning. Teknisk Rapport 1985:25 T, LuH, Sverige. 59p.

[10] Sun Z, 1983. Fracture Mechanics and Tribology of Rocks and
     Rock Joints. Doctoral Thesis, 1983:22 D, LuH, Sweden. 207p.

[11] Swan G, 1977. The Mechanical Properties of Rocks in Stripa,
     Kråkemåla, Finnsjön and Blekinge. KBS-48, prepared for
     Kärnbränslesäkerhet, Stockholm, Sweden.

[12] Swan G, 1978. The Mechanical Properties of Stripa Granite.
     Tecnical Project Report No. 3. Originally part of KBS
     Teknisk Rapport 48, Kärnbränslesäkerhet (KBS), Sweden. 25p.

[13] Swan G, 1983. Determination of Stiffness and Other Joint
     Properties From Roughness Measurments, Rock Mechanics and
     Rock Engineering, Vol. 16, pp. 19 - 38.

[14] Tammemagi H Y, Chieslar J D, 1985. Interim Rock Mass Properties
     and Conditions for Analyses of a Repository in Crystalline
     Rock. Technical Report BMI/OCRD-18. 84p.

[15] Wawersik W R, 1968. Detailed Analysis of Rock Failure in
     Laboratory Compression Tests. Ph.D Thesis, Unversity of
     Minnesota.

APPENDIX 1

DETERMINATION OF SOUND VELOCITY AND DYNAMIC
PARAMETERS OF ELASTICITY FOR ROCK SPECIMENS

Introduction

The easiest way to study the dynamic properties of rock specimens
is by means of ultrasonic sound velocity measurements. In an iso-
tropic material the velocity of the shear waves, V_s and the
compression waves, V_p is the same in all directions. If the material
is linearly elastic the elastic parameters of the specimen can be
calculated from the measured velocities, V_s and V_p.

Experiments have shown that the velocity of elastic waves in a rock
material depends both on the mineral composition of the rock and
its porosity and content of microfractures. The specimens degree
of saturation does also have strong influence on the sound velocities.
Sound velocity measurements, in combination with microscopic analysis,
can be used to study the porosity of rocks.

The main purpose of the test is to determine the elastic properties
of the specimen. This is done within the elastic loading range of
each rock type.

Equipment

The equipment for measuring sound velocity in rock specimens include
the following components:

a) Two cylindrical transducers (Φ 50 x 50 mm), each containing two
    piezoelectric crystals - one for shear waves,S the other for com-
    pression waves, P. Both crystals having own frequency of 1 MHz.
    The transducers can take an eavenly distributed compressing load
    of 220 kN, equaling 112 MPa stress

b) Pulse generator/measuring unit, type PUNDIT

c) Oscilloscope with memory, type GOULD 4000

d) Switch unit to switch between P and S crystals

e) X-Y recorder to plot from the oscilloscope memory

f) Loading machine for loading specimen and transducers to acertain good rock-transducer contact. An INSTRON 10 ton servo-hydraulic press serves this purpose.

g) Spherical seat for eaven load distribution on transducers and specimen

Figure 1 shows the principles of component layout for the test.

X- Y- RECORDER
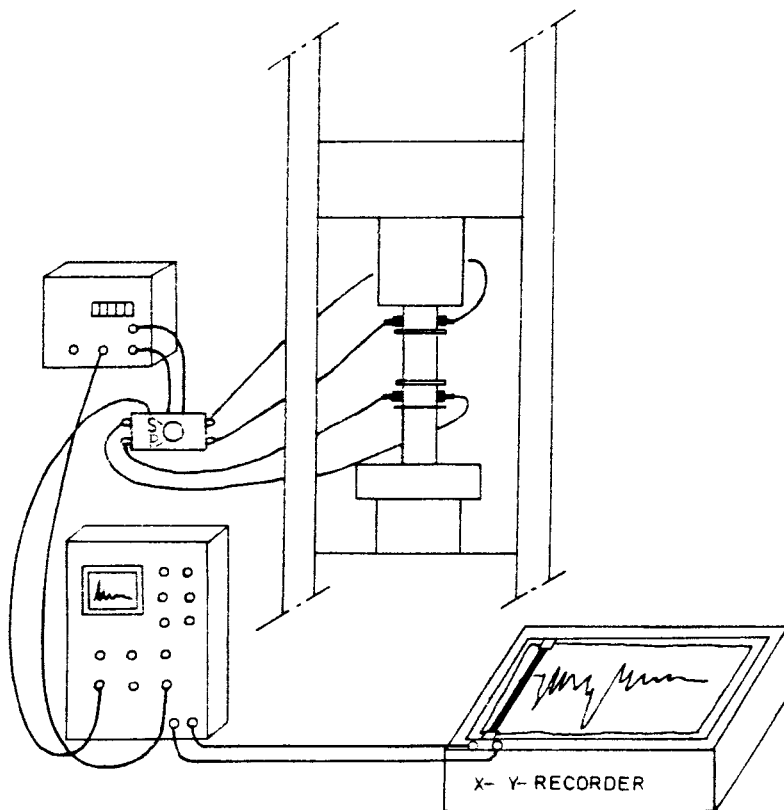
Fig. 1   The layout of components for measuring sound velocity in rock specimens.

Sample preparation

In a standard test the sound velocities, Vp and Vs, are measured
in rock specimens of straight circular cylinders. Other sample
shapes are possible but the specimen must have two parallel and
planar surfaces for placing the transducers on. It is common
to do sound velocity measurements on specimens prepared for uni-
axial compression test. These specimens meet all requirements
set on sample preparation for sound velocity tests. Test specimens
from drill cores are prepared in the following way:

a) Cylindrical specimens with parallel end surfaces are cut with
a diamond blade. The ends shall not depart from perpendicularity
to the axis of the specimen by more than 4 min or 0.05 mm over
a specimen of 50 mm diameter. As a standard we have chosen a
specimen length of 2.5 times it's diameter. The length to dia-
meter ratio should not be less than 2. An eventual departure from
this rule shall be noted in the test report.

b) After cutting the specimen it is dried in oven at 50^0 C for a
minimum period of 24 hours. The specimens are stored in a
desiccator till the time of testing.

If a specimen is to be tested in a saturated state it must
lie submerged in water for at least 24 hours before testing.
If a specimen has started drying it shall be placed in vacuum
to get rid of air in pores, preventing water to enter. After
de-airing the specimen it is submerged in water while still in
vacuum. The procedure is called vacuum impregnation.

Specimens to be tested at normal laboratory humidity shall stand
uncovered in the laboratory for one week at least.

Test procedure

The piezoelectric crystals are embedded in the steel cylinders of the transducers. While traveling between crystals on opposite ends off the specimen a sound wave must therefore pass through two layers of steel of unknown thickness plus the specimen. Before running the test we need to know the travel time of sound waves through these steel layers. This is done by placing the transducers against each other, with two pieces of double aluminium foil between, those sitting at the ends of the specimen during normal testing. The travel time through the transducer system is now measured in usual way. This procedure is called zero-reading. The travel time obtained in the zero-test will be subtracted from the total travel time during normal rock specimen testing.

Specimen and transducers must be loaded to give good acoustic contact. Experiments have shown that 5 MPa stress is sufficient to aquire good contact between specimen and transducers (see Fig. 2). ISRM's "Suggested Methods" (Brown 1981) recommend 0.1 MPa but this stress is to low for our type of transducers.

For soft rock or fractured the stress may be reduced from 5 MPa down to 3 MPa for example. In such case it should be noted in the test report. The measurements are run in the following way:

a)   Components are connected and tested

b)   Zero-reading is carried out. Travel time through the zero-system is measured both for P and S waves

c)   A rock specimen, with double aluminium foil covering each end, is now placed between the transducers

d) Specimen with transducers is now placed on a spherical seat in the press and centered carefully. The spherical seat will contribute to an eaven load distribution in the system. Specimen and transducers is now loaded to 5 MPa

e) The test is run at 5 MPa axial stress. The equipment are connected in such a way that the pulse activating the transmitting crystal will also trigger the scanning of the oscilloscope. The scanning time is chosen to give good resolution over the period from transmitting to receiving the wave. The curve on the oscilloscope is recorded by an internal memory for later plotting it on paper by a recorder working in X-t mode. The memory can save one curve at a time. Figure 3 shows typical curves for P- and S-waves and how the traveling time for these is determined. The time difference between the points on the curve is 0.55 μs. Calibration of the time axis on the paper plot is achieved by measuring the distance between points n and n + 50

f) The load is now decreased down to axial stress of 1 MPa. Measurements are repeated at this stress level

g) New double aluminium foils are placed on the ends of the specimen and points c) to f) repeated

h) Travel times through the specimen for P-waves, t_p^S and S-waves, t_s^S are found as the difference between total travel times, t_p^T and t_s^T respectively and the zero-times, t_p^0 and t_s^0 e.i.

$$t_p^S = t_p^T - t_p^0$$

$$t_s^S = t_s^T - t_s^0$$

Where t_p^T, t_s^T, t_p^0 and t_s^0 are average values from two measurements.
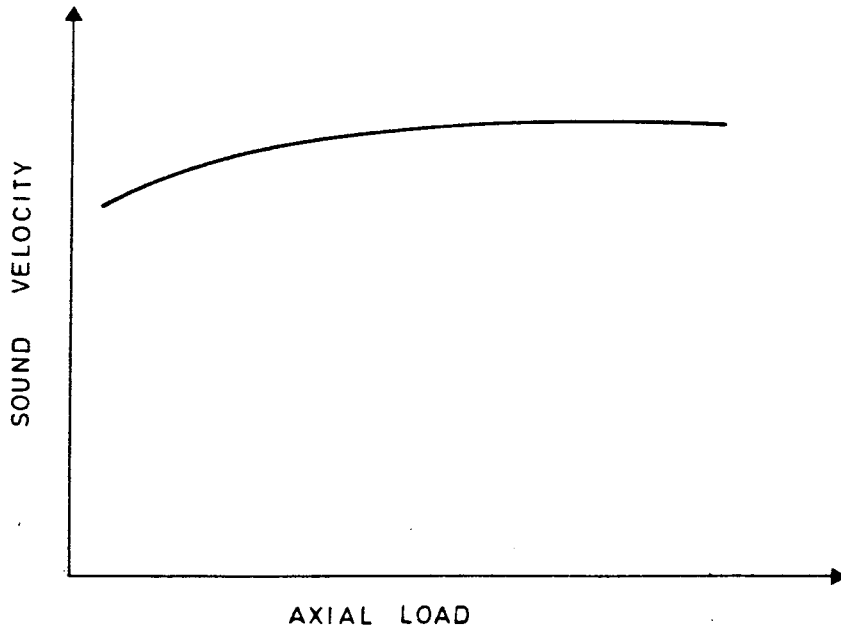
Fig. 2   Sound velocity as a function of axial stress for cylindrical
         specimens of Stripa Granite.
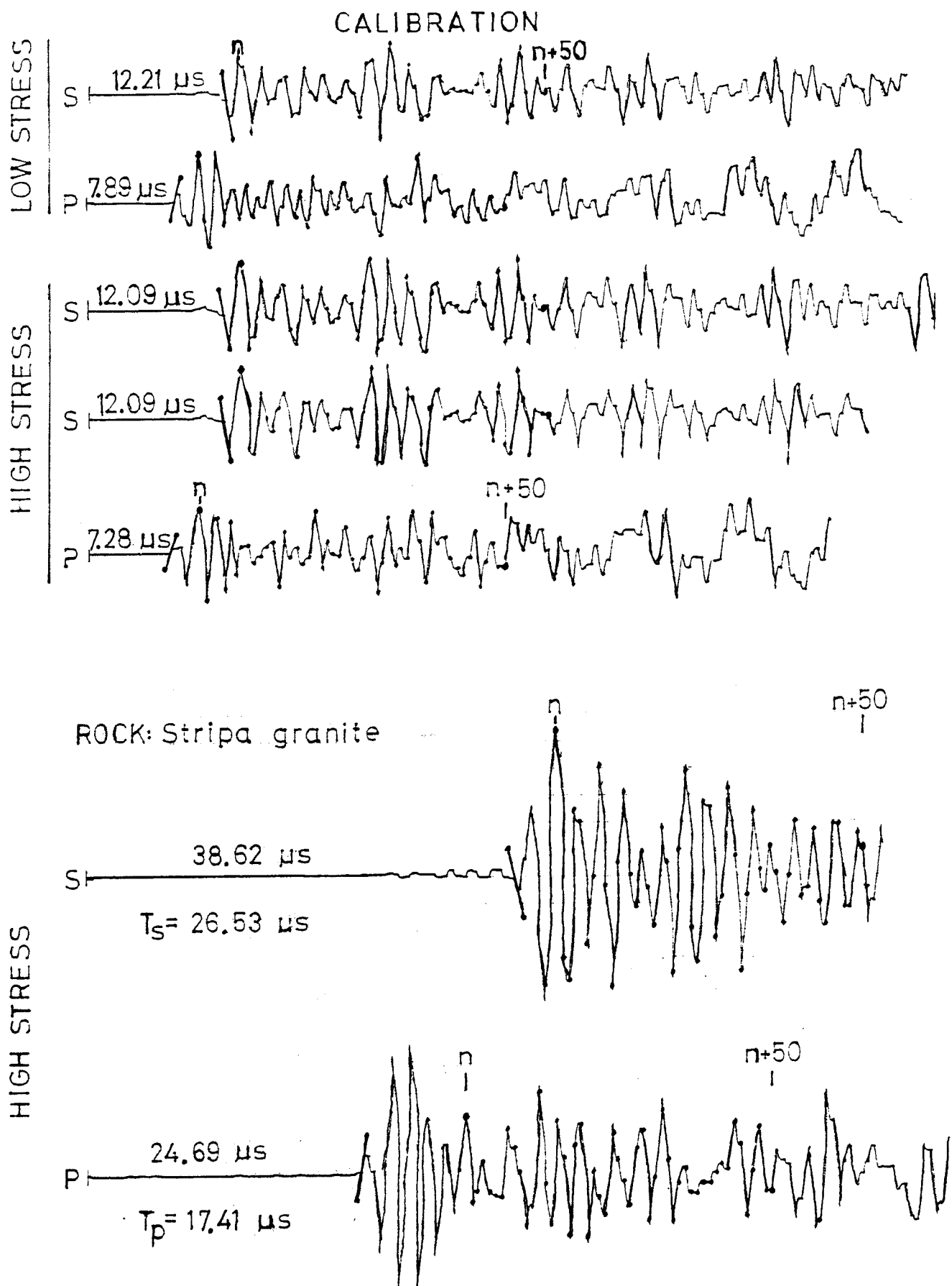
Fig. 3   Typical plots from P- and S-waves in Stripa Granite.

Calculations

For calculating the sound velocities the specimen length must be
known. In our standard tests we measure the length, L the diameter,
D and the weight, m of the specimen. The value presented for each
parameter is an average from several measurements.

Sound velocities are calculated from equations (1) and (2):

P-wave velocity $\qquad V_p = L/t_p^s$ $\qquad\qquad\qquad\qquad$ (1)

S-wave velocity $\qquad V_s = L/t_s^s$ $\qquad\qquad\qquad\qquad$ (2)

If the rock material is taken to be linearly elastic and isotropic
the elastic parameters can be calculated straight foreward. Young's
modulus, E_d and Poisson's ratio, ν_d are then found from equations (3)
and (4):

Young's modulus $\qquad E_d = \dfrac{V_s^2\, \rho\, \left[3\left(\dfrac{V_p}{V_s}\right)^2 - 4 \right]}{\left[\left(\dfrac{V_p}{V_s}\right)^2 - 1 \right]}$ $\qquad\qquad$ (3)

Poisson's ratio $\qquad \nu_d = \dfrac{1}{2}\,\dfrac{\left[\left(\dfrac{V_p}{V_s}\right)^2 - 2 \right]}{\left[\left(\dfrac{V_p}{V_s}\right)^2 - 1 \right]}$ $\qquad\qquad$ (4)

The bulk modulus, B_d and the shear modulus, G_d are found through
the relationship between E, υ, G and B. Equations (5) and (6) give
B and G as functions of E and υ.

$$B = \frac{E}{3(1 - 2\nu)} \tag{5}$$

$$G = \frac{E}{2(1 + \nu)} \tag{6}$$

<u>Reporting of results</u>

The results are listed in a table (see Table 1) and in a sample-comparison diagram (Fig. 4). Visible structures in specimens are noted in the Comment column.

Table 1 Results from sound velocity measurements, average values
from two measurements.

Rock type	Sample nr	L (mm)	ϕ (mm)	m (g)	ρ (kg/m^3)	V_p (m/s)	V_s (m/s)	E_d (GPa)	ν_d (m/s)	Comments
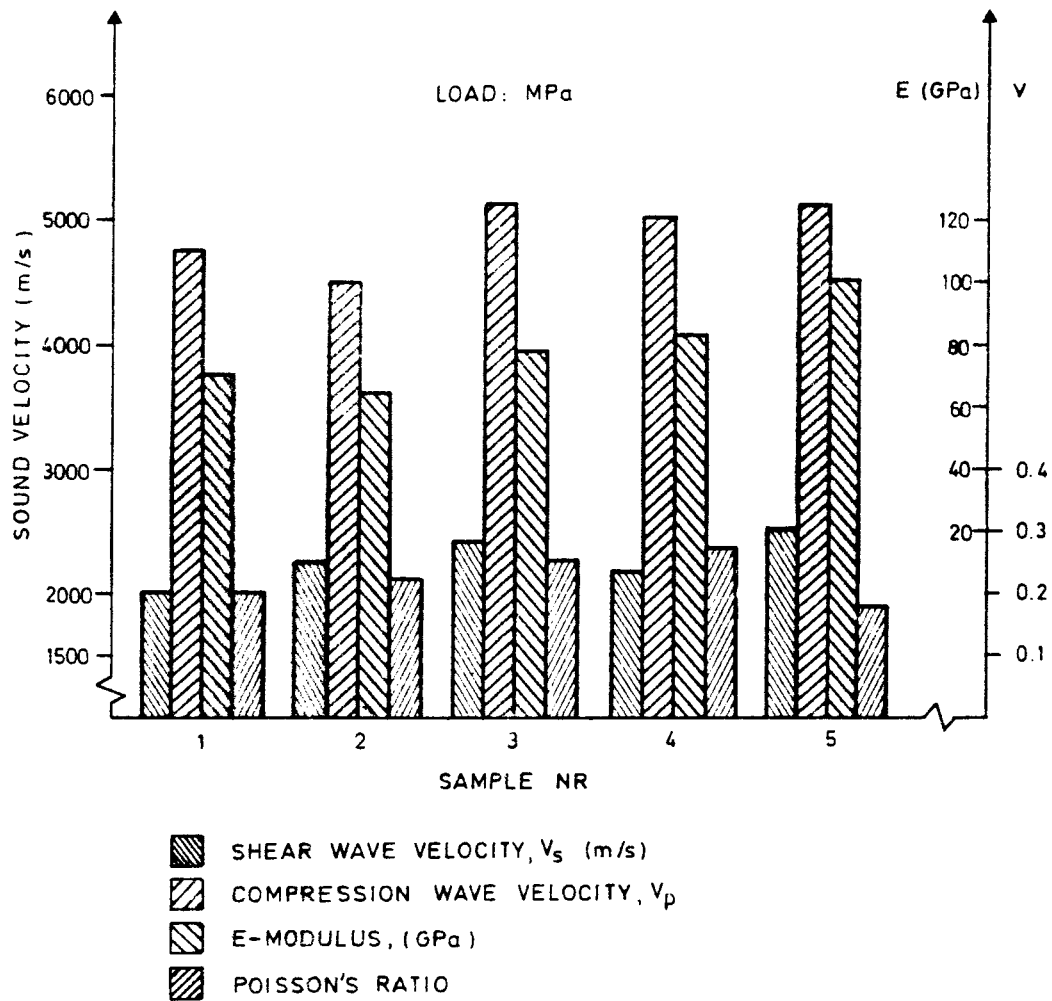
Fig. 4   Sample comparison diagram for each specimen showing: V_s
(m/s), V_p (m/s), Young's modulus (GPa) and Poisson's ratio.

References

Brown, E. T. (ed) 1981. ISRM Suggested Methods. Rock Characterization, Testing and Monitoring. Suggested Methods for Determining Sound Velocity. Pergamon Press, Oxford.

APPENDIX 2

UNIAXIAL COMPRESSION STRENGTH, MODULUS OF ELASTICITY
AND POISSON'S RATIO

This testing method serves to determine the modulus of elasticity, the Poisson's ratio and the uniaxial compression strength of intact rock samples. The test specimen is made of a rock cylinder with the ends cut perpendicular to the axis of the cylinder and polished for a high degree of parallelity. This is a standard test for determining mechanical properties of rocks.

Equipment

a) The test is run in a servo-hydraulic Instron press with loading capacity of 4500 kN and a maximum piston movement of $\pm$ 35 mm. The loading rate can be set within wide limits. The stiffness of the press is sufficiently high to neglect it's effect on the test result

b) Cylindrical platens of high quality steel are placed on both ends of the specimen. The diameter of the platens is D to D+2 mm, where D is the diameter of the specimen and the minimum thickness should be at least 15 mm or D/3. Surfaces of the platens should be ground and their flatness should be better than 0.005 mm

c) One of the two steel platens contains a spherical seat. The spherical seat must be cleaned thoroughly and lubricated by a few drops of mineral oil before placing it under the specimen. The specimen, the steel platens and the spherical seat must be accurately centered in the press before starting the test

d) Strains in the specimen during the loading cycle are measured by strain gauges. If strains are measured by some other method it's reading limits should be 5 x 10-6 strain at least.

Recommended effective length of strain gauges is 10 times the biggest grain size of the rock sample with an upper limit at half the diameter of the specimen

e) Recording of strain and load during the test may either be done by a conventional X-Y recorder or a computer

A = STEEL PLATE
B = ROCK SAMPLE
C = SPHERICAL SEAT
D = APPLIED AXIAL LOAD
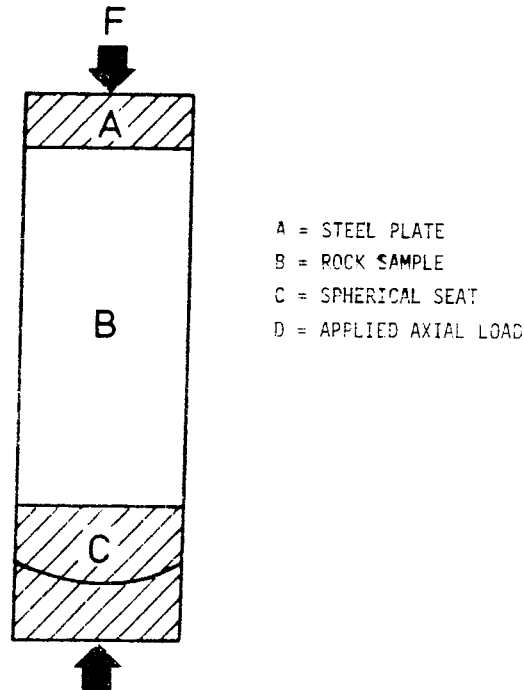
Fig. 1   Example of an experimental set-up.

Procedure

a) The rock specimen is a straight, circular cylinder with a length to diameter ratio of approximately 2.5. Smaller sample diameter than 40 mm should be avoided

b) The ends of the specimen shall be flat to 0.02 mm and shall not depart from perpendicularity to the axis of the specimen by more than 0.05 mm

c) The sides of the specimen shall be smooth and free from abrupt
   irregularities. A specimen that does not fullfil the above
   listed rules on specimen quality shall not be tested as it might
   affect the test results

d) The diameter of the test specimen shall be measured to the nearest
   0.1 mm. Three measurements shall be taken and averaged. The ave-
   rage is used to calculate the cross-sectional area of the speci-
   men. The specimen length is measured to the nearest 0.1 mm.
   Specimen weight is determined to calculate it's density. The
   weight should be measured to the nearest 0.1 g for specimen dia-
   meter of 40-80 mm

e) The axial loading rate should be set to reach specimen failure
   within 5 - 10 minutes. Alternatively a constant stress rate
   can be set between 0.5 - 1.0 MPa/s

f) The maximum load on the specimen shall be recorded in Newtons
   (or an appropriate multiple thereof) to within 1 %. The de-
   formations in the specimen are recorded in strains or a multiple
   thereof. The most common unit is the micro strain (μs)

g) As a compliment to the standard method of testing the registration
   of acoustic emission from the specimen can be acieved. This has
   shown to give valuable information on the initiation of failure
   in the specimen

h) The minimum number of specimens tested for each rock type should
   be five

Calculations

a) Axial strain is calculated from the equation:

$$\varepsilon_a = \frac{\Delta l}{l_0}$$

where ε_a = Axial strain

l_0 = Initial axial length of specimen

Δl = Change in measured axial length

b) Radial strain is calculated from the equation:

$$\varepsilon_r = \frac{\Delta d}{d_0}$$

where ε_r = Radial strain

d_0 = Initial diameter of specimen

Δd = Change in diameter

c) The axial stress in the specimen (σ) calculated from the equation:

$$\sigma = \frac{F}{A}$$

where σ = The compressive stress

F = The axial force

A = The initial cross-sectional area of the specimen

The uniaxial compression strength (σ_c) is calculated from the above equation from the maximum load on the specimen (F_{max}).

d) A typical plot from this test is shown in Fig. 2. The curves show axial stress vs. axial and radial strain in the specimen.

The diagram shows a typical behaviour of rock material through the applied stress range.
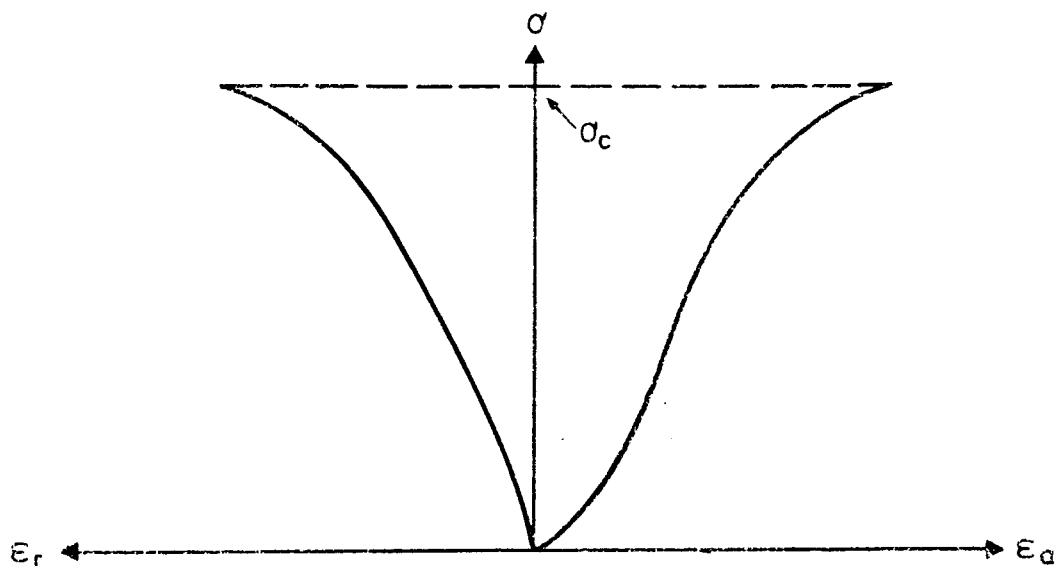
Fig. 2   Example of a graphical presentation of axial and radial stress-strain curves.

e) The modulus of elasticity is calculated from the equation:

$$E = \frac{\Delta\sigma}{\varepsilon_a}$$

where   E = The modulus of elasticity

$\Delta\sigma$ = Change in axial stress

ε_a = Change in axial strain

Various methods are accepted for calculating the modulus of elasticity. Following methods are used at the Division of Rock Mechanics:

1) The tangent modulus (E_t); calculated at 50 % stress level of the uniaxial compression strength (σ_c).
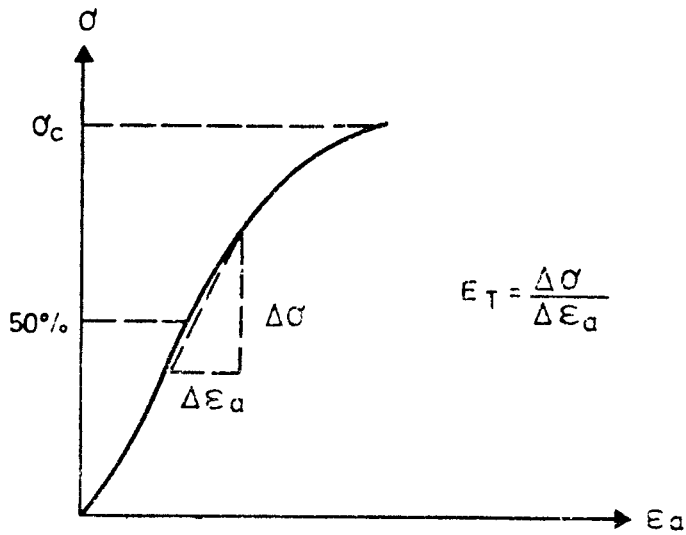
Fig. 3   Calculation of the tangent modulus of elasticity.

2) The average modulus (E_{av}); Calculated as the inclination of the linear portion of the stress-strain curve.
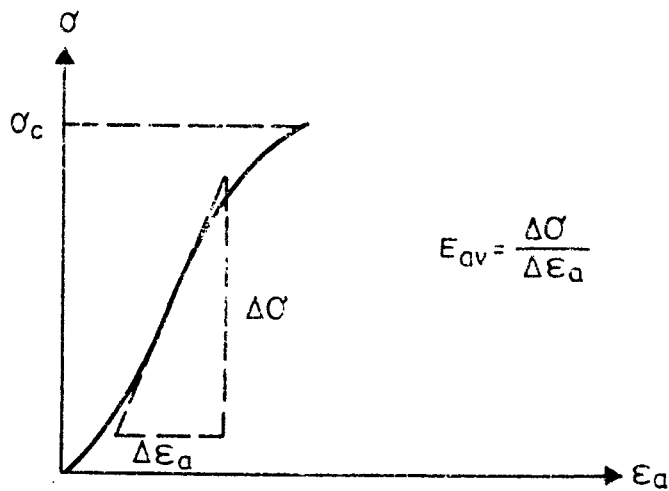
Fig. 4   Calculation of the average modulus of elasticity.

3) The secant modulus (E_s); calculated as the inclination
of the secant line to the curve from 0 point up to a fixed
percentage, commonly 50 %, of the ultimate strength (σ_c).

$$E_s = \frac{\Delta\sigma}{\Delta\varepsilon_a}$$
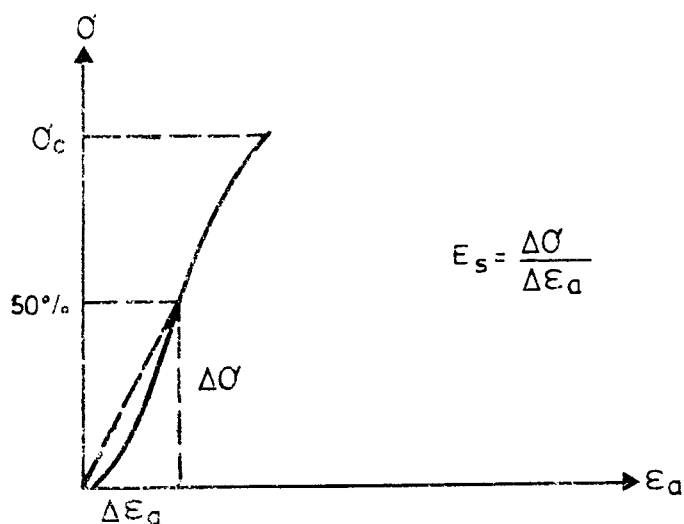
Fig. 5   Calculation of the secant modulus of elasticity.

4) The initial modulus of elasticity (E_{ini}); calculated as
inclination of the tangent to the initial part of the
curve.

$$E_{INI} = \frac{\Delta\sigma}{\Delta\varepsilon_a}$$
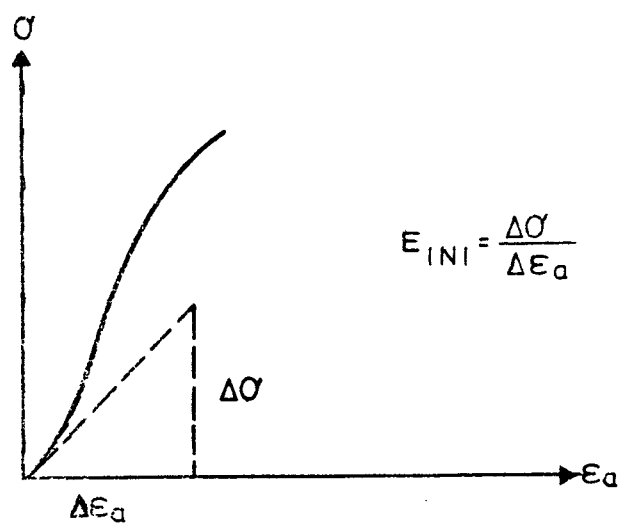
Fig. 6   Calculation of the initial modulus of elasticity.

The Young's modulus is presented in the Pascal unit (Pa) or a multiple thereof. Commonly in GigaPascals (GPa).

f) The poisson's ratio (ν) is calculated in the following way:

$$\nu = \frac{\text{Inclination of the axial stress-strain curve}}{\text{Inclination of the radial stress-strain curve}}$$

$$= \frac{E}{\text{Inclination of the radial curve}}$$

g) The volumetric strain (E_v) is calculated from the equation:

$$\varepsilon_v = \varepsilon_a + 2\varepsilon_r$$

Reporting of results

A report from the test should include the following:

a) A lithological description of the rocks tested, also giving sampling location and depth

b) Orientation of the axis of loading with respect to specimen anisotropy

c) The test results shall be set up in a table, eventually completed by a sample-comparison diagram showing the variation in compressive strength between the specimens (se figs. 7 and 8)

Rock type	Sample nr	D (mm)	L (mm)	m (kg)	ρ (kg/m^3)	F_{max} (N)	σ_c (Pa)	E_{init} (GPa)	E_{50}	ν_{in}	ν_{50}	Remarks

Fig. 7 Example of a table for test results.
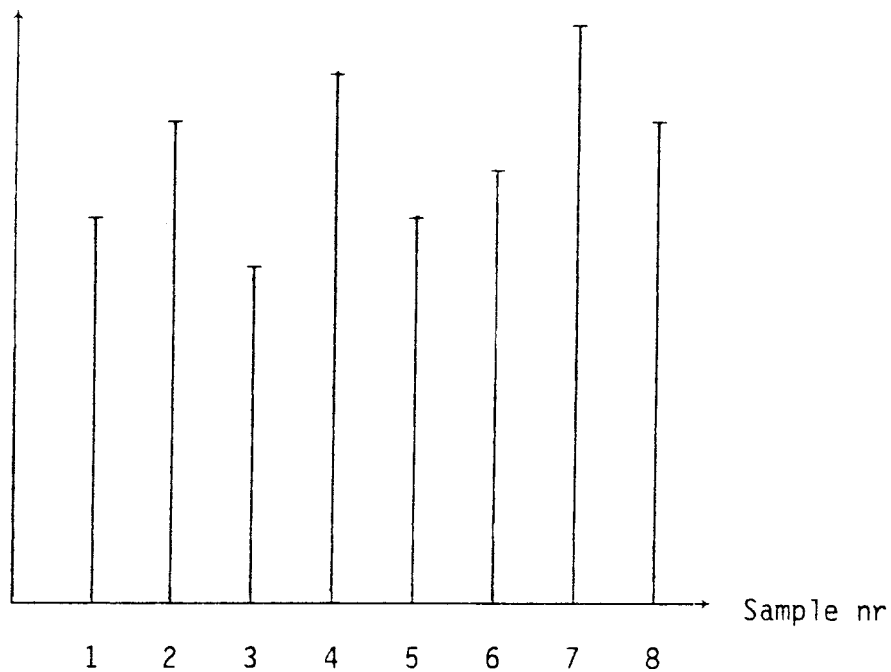
Fig. 8   Example of a sample-comparison diagram showing the variation
          of compressive strength between specimens in the same series.

References

Brown. E.T. (ed) 1981.   ISRM Suggested Methods.   Rock Characteri-
      zation, Testing and Monitoring.   Suggested Methods for Determining
      the Uniaxial Comnpressive Strength and Deformability of Rock
      Materials.   Pergamon Press, Oxford, 211 pages.

Jaeger, J.C. and Cook, N.G.W. 1979.   Fundamentals of Rock Mechanics.
      Third edition.   Chapmann and Hall, London, 593 pages.

APPENDIX 3

ACOUSTIC EMISSION

Scope

Acoustic emission are used as a help and complement to other test
methods wich are conducted at the Division of Rock Mechanics,
Technical University of Luleå. By the acoustic emissions one
registeres the sound waves caused by crack generation in a rock
sample. The acoustic emissions are used to get an idea about when the
cracks initiate and propagate. At the present the acoustic emissions
(AE) can be used as a routine in the following testing methods:
Uniaxial compression test, three point bending test, brazilian test,
as well as hydraulic fracturing and sleeve fracturing.

Apparatus

The equipment for acoustic emission consists of the following parts:

1) Transducer: A piezoelectric transducer which is in contact with the
   sample and transforms the sound waves of the microcracking into
   electrical signals.

2) Pre-amplifier: It is placed near the transducer and transfers the
   signal to the counter. The amplification is +60 dB.

3) Filter: It filters out mechanical (low frequence) and electromag-
   netic disturbances. The signals which are significant for rock are
   within the frequency range 100 kHz - 1 MHz.

4) Amplifier: It amplifies the signal even more. The amplification can
   be varied between 0-60 dB in steps of 1 dB.

5) Threshold detector: The instrument reads the signal and only
   releases the peaks which pass over a pre-set threshold value.

6) Counter: Counts the number of pulses that have passed the threshold
   detector.

Besides, a printer can be connected, which will then show the acoustic emissions.

Procedure

The AE equipment is connected according to the block diagram below, Fig 1:

TRANS-   PREAM-   FILTER   AMPLIFIER   THRESHOLD-   COUNTER
DUCER   PLIFIER   DETECTOR
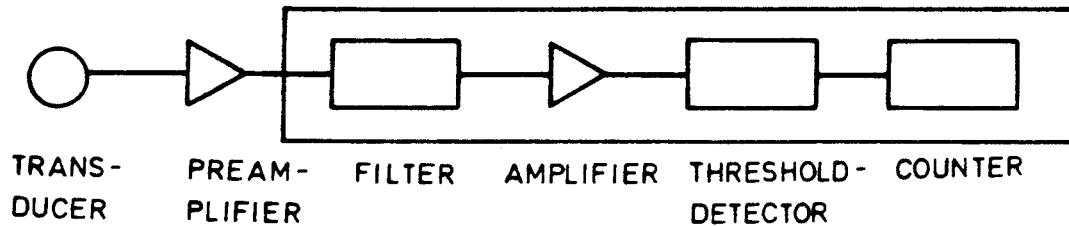
Fig 1   Block diagram for AE equipment.

The transducer (phone) is placed as close as possible to the sample, but not so near that eventual rock splinters can damage it. In uniaxial compression test, the transducer is placed in a specially constructed holder so that it is well protected. The holder is placed directly under the sample. Between the metal surface and the transducer is applied a thin layer of vacuum grease. This is to improve the transfer of signal to the measuring instrument and to avoid the registration of not wanted signals.

A micro-computer of type ABC 800 is connected to the counter for the collection of the acoustic emissions during the test. The frequence interval is set to 300 kHz - 1 MHz.

Calculations

The acoustic emissions do not give any value of a rock's strength or elastic paramenters. AE shall be seen as a complement to the other testing methods. What AE can show is how fast and at which load the cracks initiate and propagate.

Presentation of results

The results of AE is presented in the form of curves, where the registered AE are plotted as a function of load: The curves can be presented in four different ways:

1) The sum of the number of pulses that the counter has registered since the sample was loaded.

2) The appearance of the second curve depends to a great extent on the chosen time basis. The counter sums the same pulses as it did in the case of the first curve, but with the exception that the recording takes place at the end of every time period. In our equipment the following time periods are available :

   1/10 s, 1/5 s, 1 s, 2 s, 10 s, 30 s, 1 min, 2 min and 20 min

3) In the third alternative, Fig 4, all the pulses in the time period chosen are summed. After every time period, the counter is reset and starts counting from zero. This curve gives a clear idea of the microcracking activity in the sample. This can be useful because it is known that the activity increases strongly when the stresses in a sample get close to the failure limit.

4) The last alternative, Fig 5, is a clearer version of method nr. 3. Here, all the pulses under the set up time period are summed. At the end of the time period, the sum is written down, at the same time as the counting has been set to zero and started counting the pulses in the following period.
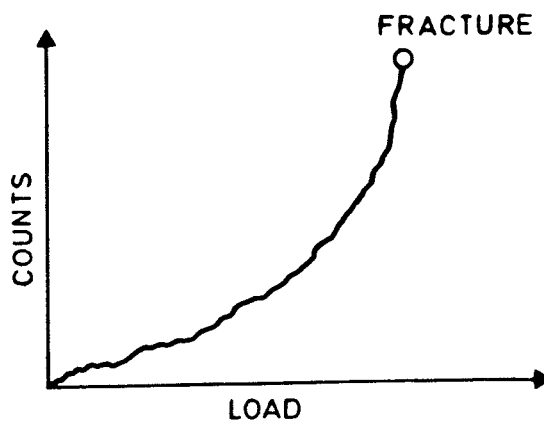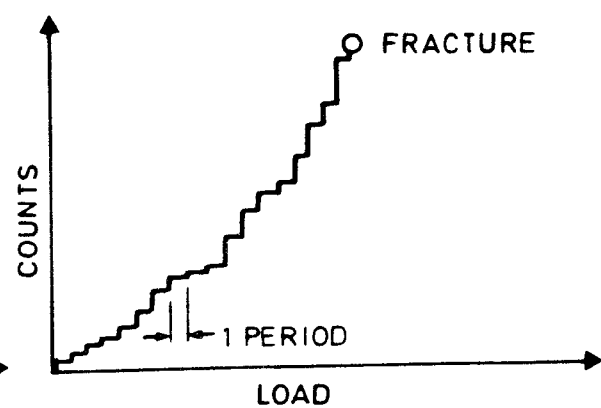
Typical curve alt. 1   Typical curve alt. 2

4
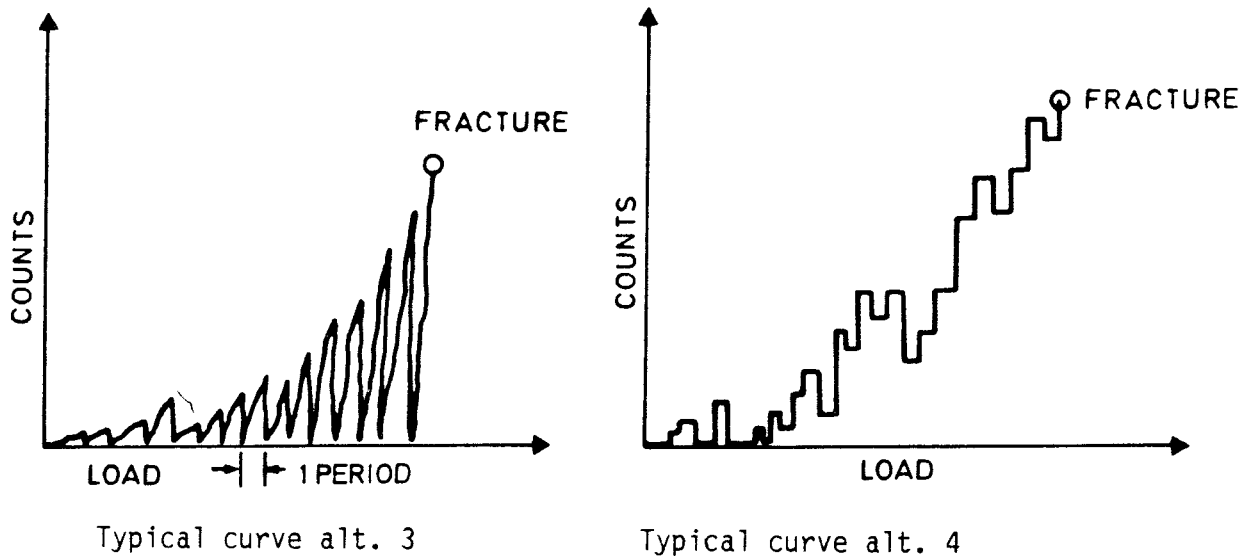
Fig 2   Typical curves for the different registering alternatives.

References

Ljunggren, C. 1984. Laboratoriebestämning av bergarters draghåll-
fasthet med hydraulisk spräckning och membranspräckning.
Examensarbete 1984:078 E. Högskolan i Luleå, Luleå.

Ljunggren C, Norin J, 1985. Akustisk Emission Vid Bergartstestning.
Teknisk Rapport 1985:25 T. Högskolan i Luleå, Luleå.

APPENDIX 4

DETERMINATION OF INDIRECT TENSILE STRENGTH WITH BRAZILIAN TEST

Apparatus

a) A loading rig consisting of two steel plates loads a disc shaped
   rock specimen diametrically, until failure occurres, see Fig 1. The
   dimensions of the parts of the loading rig are the following: The
   radius of the steel plates is 1.5 x the radius of the specimen, the
   guide pins permit a rotation of one jaw relative to the other by
   4×10^{-3} radians out of plane of the apparatus. The width of the
   jaw is 1.1 x the specimen's thickness. The upper steel plate (jaw)
   has a spherical seat to avoid inclined loading.

b) A servo-hydraulic Instron press is used to load the specimen in a
   controlled manner.

c) An X - Y recorder is used to register the load.
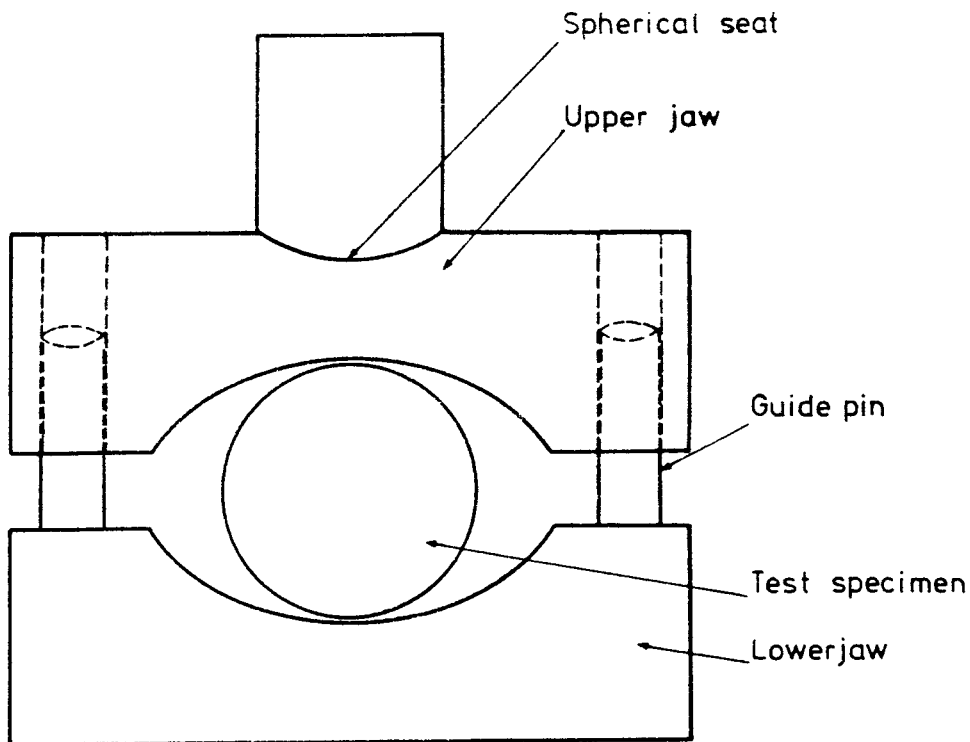
Fig 1   Loading equipment for Brazilian test.

Procedure

a) The specimen is cut, so as to provide parallel ends.

b) The diameter of the specimen is normally 42 mm, and the thickness is chosen to be 0.5 x the diameter.

c) The orientation of the specimen shall be known and is given in the results table.

d) The specimen is placed so that the load is applied diametrally.

e) The loading rate is chosen so that failure occurres within 15 - 30 seconds.

f) The load is registered continously on the X - Y recorder, and the failure load is estimated.

g) The number of samples varies depending on the practical circumstances. Since the results often show a large spread, the number of specimens should be at least 10 for each rock type.

Calculations

The tensile strength, σ_t, is calculated with the following formula:

$$\sigma_t = 0.636 \ P/D \ x \ t \ (MPa)$$

where
P = failure load (N)

D = diameter of the specimen (mm)

t = thickness of the sample (mm)

Presentation of results

a) Description of specimen location and depth.

b) Geological description of the rock type.

c) Orientation of anisotropy or foliation in relation to the direction

of the load.

d) Description of the failure appearance for each specimen.

e) Tests results are presented tabulated, according to Table 1

Table 1   Tensile strength by Brazilian test method.

Rock type	Sample nr	Dia meter D [mm]	Thickness t [mm]	Mass m [g]	Density ρ [kg/m^3]	Max load F_{max} [N]	Tensile strength σ_T [MPa]	Remarks

References

Mellor, M. och Hawkes, I. 1971. Measurement of tensile strength by
   diametral compression of disces and annuli. Eng Geol, 5, pp
   173-225.

APPENDIX 5

CONTROLLED TRI-AXIAL COMPRESSION TESTING

Purpose

It is known that natural rock formations are in a tri-axially state of stress. Knowledge of the strength of rock under such state is very important for designing structures in rock.

By conducting conventional tri-axial tests, it is possible to obtain the strength of rock under different confinements. These data further help us to determine the strength envelope and calculate the internal friction angle (Φ) and 'apparent' cohesion (c) of the rock material.

Controlled tri-axial testing, however, are more informative. They show us how rocks behave when their peak strengths have been passed and how reduction in load-bearing capacity takes place with the continuation of deformation.

Testing equipment

A high pressure cylindrical vessel, with a pressuring chamber diameter of 70 mm and height of 170 mm, made of handened steel is used. Strain gauge wires are connected to a specially designed collar, sitting at the bottom of the chamber. The teflon packing ring of the collar seals of the oil from leaking out. Details of the vessel and accessories are found in Fig 1, schematically.

A pressure intensifier provides the necessary confining pressure and maintains the pressure constant, while the specimen is being deformed.

The axial load on the sample is applied by the existing 4500 kN stiff and servocontrolled Instron testing machine. It is possible to carry-out the test in 'strain control' by this system. Details of the system is shown schematically in Fig 2.
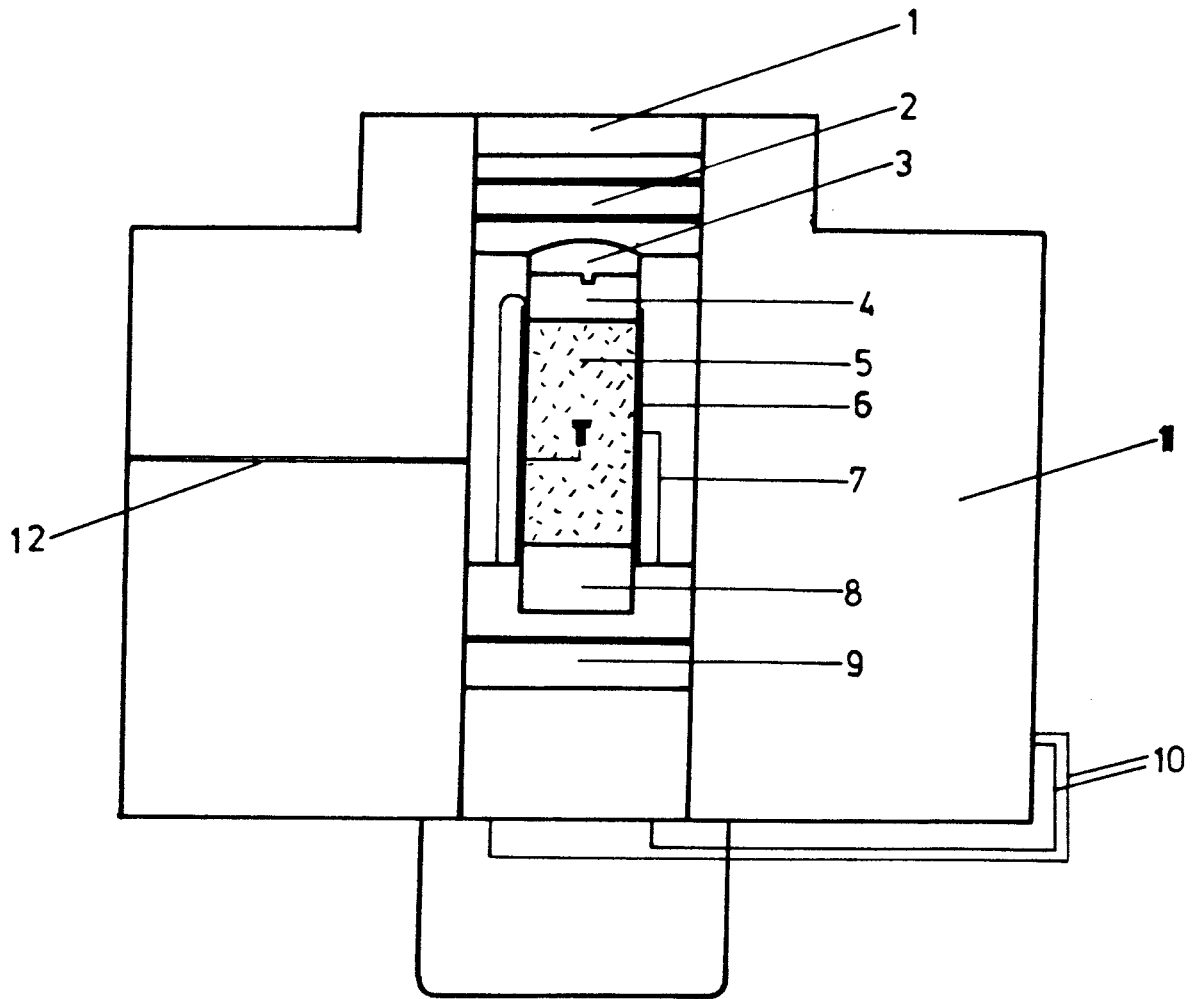
Fig 1   Schematic view of the high pressure vessel, accessories and
         the sample

1 - Pressurizing chamber

2 - Top piston with two teflon
    Packing rings

3 - Sperical seat

4 - Top platen

5 - Specimen

6 - Sleeve

7 - Inside wires

8 - Bottom platen

9 - Bottom collar with one
    teflon packing ring

10 - Outside wires

11 - Body of the vessel

12 - Oil duct
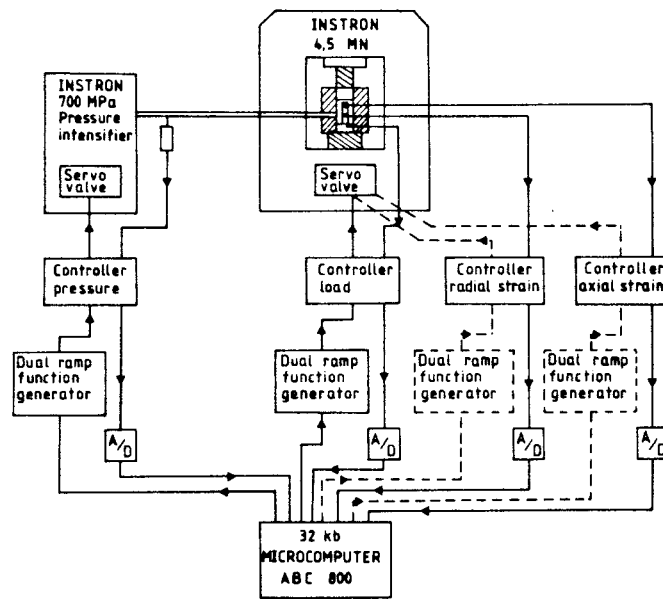
Fig 2   Schematic view of the 4500 kN Instron Press

Fig 3   A prepared specimen for tri-axial testing

Specimen preparation

Samples of the rock to be tested, with diameter of 41.5 ± 0.5 mm and length to diameter ratio of L/D = 2 are prepared for testing. The preparation is exactly as that for uniaxial testning with longitudinal and circumferential strain gauges mounted on the specimen for strain measurements. The specimens are then prowided with 'Cast on Rock Inclusion Gauged Sleeves', so that controlled tri-axial testing can be carried out on them. Two long strain gauges are embedded in these sleeves and provide the 'feedback' signal for the loading system. Details of the sleeve preparation is reported elsewhere [3]. Fig 3 shows a prepared specimen.

Testing procedure

The experiments are conducted in the following way:

- The specimen is placed in the pressurizing chamber, all the strain gauge wires are connected and the chamber is filled with oil.

By pushing the top piston into the chamber, the specimen is slightly loaded, while no oil pressure is being built up.

- The confining pressure is raised to the desired value by the pressure intensifier.

- The loading of the specimen, then starts in `position control', (see reference 2).

- At about 50% of the ultimate strength of the specimen, the control is transferred to `strain controller' module, where the long circumferetial strain gauges are responsible of prowiding the `feedback' signal for the system.

- The experiment is continued in this manner until the complete load-deformation curve for the specimen is recorded.

Calculation of the elastic properties

Calculations of the fracture stress, modulus of elasticity, axial and radial strains are exactly as those for uniaxial testing.

Reporting of the results

A summary of the results may be reported in a table, an example of which is given below.

Sample No	Confining pressure MPa	Fracture stress MPa	Young's modulus GPa	Failure description

REFERENCES

1) Brown E.T. (ed), 1981. ISRM suggested Methods, Rock Characterization, Testing and Monitoring.

2) Instron Manuals

3) Hakami Hossein, 1985. Cast on Rock Inclusion Gauged Sleeve for Controlled Uni-axial and Tri-axial Compression Tests on Rocks. A progress report, Internrapport BM 1985:01.

4) Wawersile, W.R. 1968. Detailed Anlysis of Rock Failure in Laboratory Compression Test. Ph.D Thesis, University of Minnesota.

APPENDIX 6

FRACTURE TOUGHNESS DETERMINATION WITH THREE POINT
BENDING TEST

Scope

With this method it is determined a rock's modulus of elasticity, E,
and the stress intensity factor, K_{IC}, which is a measure of the stress
concentration at a crack tip. The three point bending test also gives
the energy release rate, G. The test can either be performed as a one
cycle test or as a several cycles test.

Apparatus

The experimental set-up is shown in Fig. 1. The experiment is conduc-
ted in a 10 ton servohydraulic Instron press, which is equipped with
a 1.5 ton load cell for registering the applied load. Downwards
flexure at the loading point is measured with two LVDT transducers
(Linear Variable Differencial Transformer). Widening of the crack is
measured with a COD gauge (Crack Opening Displacement). An X-Y re-
corder of type Hewlett Packard 7046A is used for registering load as
function of the average value of the LVDT transducers.

SECRBB configuration
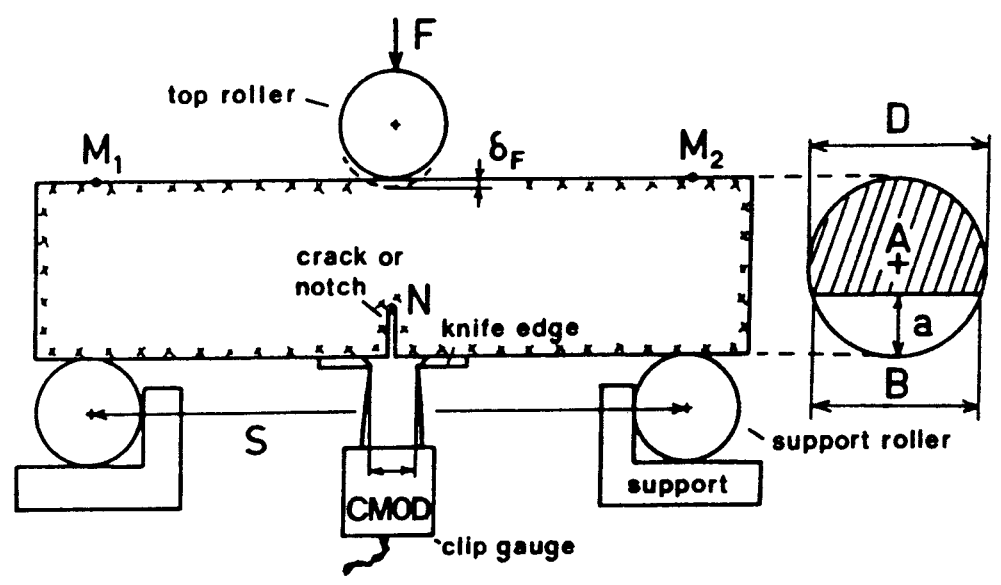
Fig 1   Experimental set-up for three point bending test.

Procedure

a) The three point bending test is conducted on drill cores and the ratio S/D shall be 3.33, where S is the c-c distance between the support rollers and D is the diameter of the core.

b) At one half of the distance S is sawn a 0.8 mm wide and 10 mm deep notch.

c) The supports for the COD gauge are glued on the sample.

d) Mounting of the measuring frame and the yoke on the sample.

e) The prepared sample is placed in the press.

f) A low load is applied to the specimen under load control, usually 0.1 KN.

g) Alignment of the specimen under load.

h) Mounting of COD gauge.

i) The measuring frame is controlled and adjusted.

j) Mounting of LVDT transducers as well as zero correction of the signals.

k) A X-Y recorder is connected to the load signal as well as to the LVDT signals.

l) The test is strain controlled via the COD gauge, with a strain rate of 0.1 μm/s.

m) The time for a test to total failure should not exceed 15 min.

Calculations

The calculations for a test with only one cycle are done according to the following:

Step 1   Calculate the initial modulus of elasticity, E

$$\lambda \times E \times D = g(a/D, \nu) = 15.6719[1 + 0.1372(1 + \nu) +$$

$$+ 11.5073 \times (1 - \nu^2)(a/D)^{2.5} \times$$

$$\times (1 + 7.0165(a/D)^{4.5})] \qquad (1)$$

where $\lambda = \dfrac{\Delta\delta F}{\Delta F}$ [mm/kN]

a = crack length [mm]. Here, it is set $a = a_0$

a_0 = notch depth [mm]

D = diameter of the sample [mm]

ν = Poisson's ratio
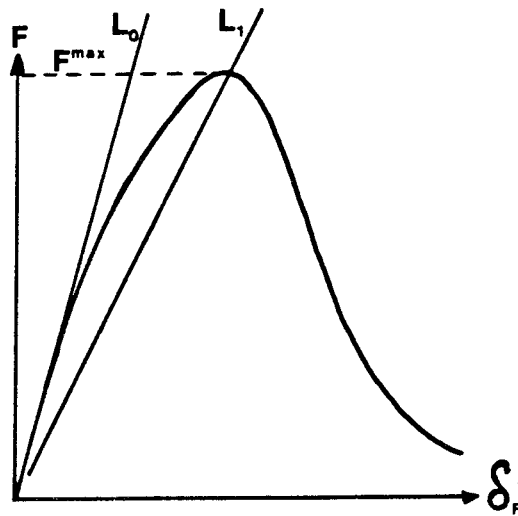
Fig 2   Diagram of load, F, as funtion of load point deformation, δ_F, for a test with one cycle.

Step 2   Calculate the real crack length, a, from equation (1) with an iterative method. Use λ from L_1 and the modulus of elasticity from the first calculation.

Step 3   Use a, given from step 2 to calculate the paramenter Y` in equation (2)

$$Y` = 12.7527(a/D)^{0.5} [1 + 19.646(a/D)^{4.5}]^{0.5}/(1 - a/D)^{0.25}$$

$$(2)$$

Step 4   Calculate fracture toughness, K, with equation (3), where
$F = F_{max}$ (see Fig 2)

$$K = 0.25(S/D) \times Y` \times F/D^{1.5} \tag{3}$$

Where $K = K_{sec}$ Secant fracture toughness $[MN/m^{3/2}]$

Step 5   Calculate energy release rate, G

$$G = (1 - v^2) \times K^2/E \ [J/m^2] \tag{4}$$

Cyclic tests

The evaluation procedure for cyclic tests is similar to that for one cycle tests. Fig 3 shows an idealized diagram of load as function of load point deformation from a several cycle test.
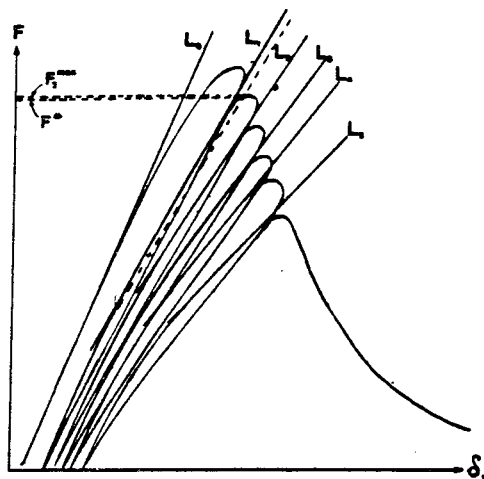
Fig 3   Diagram of load, F, as function of load point deformation, δ_F, for a cyclic test.

The lines L_1 - L_4 in Fig 3 are drawn through the linear portion of the curves from cycles 2 - 5. The stepwise calculation for curves like the

one above, is described below.

Step 1 Identical to Step 1 for one cycle tests.

Step 2 Use equation (1) to calculate the real crack length, a, after
the first cycle. Use λ from line 2 and the modulus of
elasticity, given from Step 1, as E

Step 3 Identical to Step 3 for one cycle tests.

Step 4 Calculate fracture toughness, K, with equation (3). S is the
distance between the support rollers and D is the diameter of
the specimen. Y` is given in Step 3. There are at least two
ways to estimate the force F. The first way to do it is to
draw a line with a slope which is 5 % less than the slope of
line 1 (the dashed line in Fig 3) and use the value where the
line crosses the curve, as the force. The other method is to
use the maximum force for cycle 2, F_2^{max} , as F in equation
(3). We recommend the latter method.

Step 5 Repeat Step 1 to Step 4 for the following cycles.

Step 6 Calculate the man value of the values obtained in step 1
through step 5.

The calculated fracture toughness values in Step 1 to Step 5 are
called K_{cyc1}, K_{cyc2}, and so on, where the index indicates which cycle,
after the first failure, is behind, as basis for the calculation of
the fracture toughness. It is recommended that at least four K_{cyc}
values from four different cycles are calculated after the first
cycle. It should be pointed out that the first cycle in a cyclic test
can be used to calculate K_{sec} in agreement with one cycle tests. The
G value for every cycle is calculated according to equation (4).

Presentation of results

a) A geologic description of the rock type

b) Orientation of eventual anisotropy in relation with the direction

of loading

c) Description of the location from which the sample was taken:
   Geographic location and depth.

d) A table where all the calculated values for each sample, as well as
   the sample's diameter and notch depth are listed.

Rock type	Sample Nr	Φ [mm]	$\frac{\Delta a}{\Phi}$	ν	E [GPa]	$\frac{a}{\Phi}$	F_{max} [MN]	K [MN/m$^{3/2}$]	G [J/m^2]

Fig 4   Presentation of data from a three point bending test.

References

Ouchterlony, F. 1980. Compliance measurements on notched rock cores in
   bending. Report DS 1980:2. SveDeFo, Stockholm.

Ouchterlony, F. 1982. Fracture toughness testing of rock. Report DS
   1982:5. SveDeFo, Stockholm.

Ouchterlony, F., Swan, G. och Sun Zongqi. 1982. A comparison of
   displacement measurement methods in the bending of notched rock
   cores. Report DS 1982:16. SveDeFo, Stockholm.

Swan, G. 1980. Some observations concerning the strength-size
   dependency of rocks. Research Report TULEA 1980:01, Luleå
   University of Technology, Luleå.

List of Technical Reports

1977-78
TR 121
KBS Technical Reports 1 – 120.
Summaries. Stockholm, May 1979.

1979
TR 79-28
The KBS Annual Report 1979.
KBS Technical Reports 79-01 – 79-27.
Summaries. Stockholm, March 1980.

1980
TR 80-26
The KBS Annual Report 1980.
KBS Technical Reports 80-01 – 80-25.
Summaries. Stockholm, March 1981.

1981
TR 81-17
The KBS Annual Report 1981.
KBS Technical Reports 81-01 – 81-16.
Summaries. Stockholm, April 1982.

1982
TR 82-28
The KBS Annual Report 1982.
KBS Technical Reports 82-01 – 82-27.
Summaries. Stockholm, July 1983.

1983
TR 83-77
The KBS Annual Report 1983.
KBS Technical Reports 83-01 – 83-76
Summaries. Stockholm, June 1984.

1984

TR 85-01
**Annual Research and Development Report
1984**

Including Summaries of Technical Reports Issued
during 1984. (Technical Reports 84-01–84-19)
Stockholm June 1985.

1985

TR 85-01
**Annual Research and Development Report
1984**

Including Summaries of Technical Reports Issued
during 1984.
Stockholm June 1985.

TR 85-02
**The Taavinunnanen gabbro massif.
A compilation of results from geological,
geophysical and hydrogeological investi-
gations.**
Bengt Gentzschein
Eva-Lena Tullborg
Swedish Geological Company
Uppsala, January 1985

TR 85-03
**Porosities and diffusivities of some non-
sorbing species in crystalline rocks.**
Kristina Skagius
Ivars Neretnieks
The Royal Institute of Technology
Department of Chemical Engineering
Stockholm, 1985-02-07

TR 85-04
**The chemical coherence of natural spent
fuel at the Oklo nuclear reactors.**
David B. Curtis
New Mexico, USA, March 1985

TR 85-05
**Diffusivity measurements and electrical
resistivity measurements in rock samples
under mechanical stress.**
Kristina Skagius
Ivars Neretnieks
The Royal Institute of Technology
Department of Chemical Engineering
Stockholm, 1985-04-15